Borosilicate glass alteration in vapor phase and aqueous medium

Sathya Narayanasamy, Patrick Jollivet, Christophe Jégou, Mélanie Moskura, Abdesselam Abdelouas, Thibault Charpentier, Frédéric Angeli

ARTICLE OPEN

Check for updates

Borosilicate glass alteration in vapor phase and aqueous medium

Sathya Narayanasamy[1]✉, Patrick Jollivet[1], Christophe Jégou[1], Mélanie Moskura[2], Abdesselam Abdelouas[3], Thibault Charpentier[2]✉ and Frédéric Angeli[1]✉

A Na-alumino-borosilicate glass and its Ca-doped counterpart were altered in vapor phase (98% relative humidity) and aqueous medium at 90 °C. Both the alteration media were enriched in ^{17}O. Characterization of the altered samples pointed out some differences between glass alteration in aqueous medium and vapor phase in terms of the alteration kinetics, the effect of Ca-doping on glass chemical durability, the behavior of elements in the gel layer, and the structure of the gel layer. Some of the key results are the recondensation of boron in the gel layer formed in the vapor phase and the utility of Rotation Echo DOuble Resonance Nuclear Magnetic Resonance spectroscopy to qualitatively distinguish between signals from the pristine glass and hydrated gel layer within a sample that was not altered to the core. The results gave rise to inferences about glass alteration mechanisms in both the alteration media and the differences between them.

npj Materials Degradation (2022)6:86 ; https://doi.org/10.1038/s41529-022-00298-2

INTRODUCTION

Vitrification of high-activity radioactive waste is one of the most effective approaches for the containment of the radioactive wastes. The resulting "nuclear waste glasses" may be disposed by storage in a deep-geological repository with engineered barriers for human and environmental protection. For example, in France it is envisaged that such a repository will be constructed in the North-eastern part of the country in a Callovo-Oxfordian clay layer that is located 500 m beneath the earth's surface. In such a repository, the nuclear waste glasses might be exposed to both humid conditions and saturated conditions[1]. The evaluation of the environmental safety aspect of this disposal system strongly depends on the predictions of the long-term stability and chemical durability of these nuclear waste glasses in both conditions. Many studies have focused on the behavior and chemical durability of nuclear waste glasses of different compositions in saturated conditions (referred to as aqueous alteration in this study) within a range of experimental parameters[2–9]. Such studies have enabled us to gain a generalized understanding of the glass-water reaction mechanisms[10–17]. Some of these experimental data have been useful to develop geochemical, empirical or structure-based models to predict glass alteration rates, at least during specific alteration stages[18–24]. On the other hand, the studies investigating nuclear waste glass alteration in humid conditions (referred to as vapor hydration or vapor phase alteration) are relatively fewer[25–32]. A generalized understanding of the predominant glass alteration mechanisms in the vapor phase is yet to be achieved. The following study has been carried out within this framework.

Experimental vapor phase hydration of two borosilicate glasses has been carried out in this study, alongside aqueous alteration experiments at a very high glass surface area to solution volume (SA/V) ratio. Such a high SA/V ratio facilitates the practicality of conducting experiments with the ^{17}O isotope in the solution and having sufficient quantity of altered samples for NMR characterization.

The series of experiments in this article were carried out with the following objectives: (i) study the similarities and differences between glass alteration in vapor phase and aqueous medium at a very high SA/V ratio; (ii) compare the global structure of altered layer formed in vapor phase and aqueous medium; (iii) based on the comparison, gain further understanding of the predominant mechanisms of vapor hydration of glasses.

The two glass compositions chosen for the study are: a quaternary Na-alumino-borosilicate glass, named Q (composition in mol% of oxides, 57.5 SiO_2–15.3 B_2O_3–19.2 Na_2O–8.1 Al_2O_3) and the same glass but comprising CaO, named QCa (52.7 SiO_2–14.6 B_2O_3–19 Na_2O–7.5 Al_2O_3–6.2 CaO). This choice was based on the fact that simplified compositions facilitate the understanding of influence of specific elements, which in turn might give insights into glass alteration mechanisms. Specifically, the influence of Ca was chosen to be studied since its effect on glass aqueous alteration across different SA/V regimes and progress of glass alteration are relatively well understood[6,33–35]. This understanding might help us to gain insights into the effect of Ca in vapor phase.

Table 1 lists the series of experiments that were carried out with their main parameters. Experiments 1 and 3 are aqueous alteration experiments conducted with glasses Q and QCa respectively in a ^{17}O enriched aqueous medium. These powder samples were used for NMR spectroscopy studies for the investigation of the local environments of ^{17}O, ^{11}B, ^{23}Na, ^{27}Al and ^{29}Si in the altered samples. Experiments 2 and 4 are duplicate experiments for 1 and 3 respectively, which are useful to follow alteration kinetics. Only powder samples were used for aqueous alteration experiments to be able to impose the very high SA/V ratio. Experiments 5 and 6 are vapor phase experiments conducted with the glass Q in a ^{17}O enriched vapor phase. Powder and monolith samples were used respectively according to the characterization method used. Similarly, experiments 7 and 8 are vapor phase experiments

[1]CEA, DES, ISEC, DE2D, LCLT, Université Montpellier, Marcoule, 30207 Bagnols sur Cèze Cedex, France. [2]Université Paris-Saclay, CEA, CNRS, NIMBE, 91191 Gif-sur-Yvette Cedex, France. [3]SUBATECH, CNRS-IN2P3, IMT Atlantique-Université de Nantes, 4 rue Alfred Kastler, BP 20722, 44307 Nantes Cedex 03, France. ✉email: sathya.narayanasamy@empa.ch; thibault.charpentier@cea.fr; frederic.angeli@cea.fr

Table 1. List of glass alteration experiments.

Alteration medium	Exp. no.[a]	Glass	Sample[b]	Weight, mg	Alteration solution	SA/V ratio, m^{-1}	Characterization after alteration	Alteration duration, days
Aqueous medium	1	Q	Powder ($0.45 < \Phi < 2\,\mu m$)	253	Immersion in 2.22 mL of DI water with **40% enrichment in $H_2{}^{17}O$**[c]	570438	Solid state NMR of glass powder[d] + solution analysis (ICP-OES) on 59th day	59
	2			301	Immersion in 2.41 mL of DI water of *Natural Isotopic abundance*	626639	SEM, XRD of glass powder + solution analysis (ICP-OES) on days 7, 14, 21, 28, 56, 59	
	3	QCa		251	Immersion in 2.06 mL of DI water with **40% enrichment in $H_2{}^{17}O$**[c]	563708	Solid state NMR of glass powder[d] + solution analysis (ICP-OES) on 213th day	213
	4			299	Immersion in 2.39 mL of DI water of *Natural Isotopic abundance*	578090	XRD of glass powder + solution analysis (ICP-OES) on days 7, 14, 21, 28, 56, 108, 213	
Vapor phase	5	Q	Powder ($0.45 < \Phi < 2\,\mu m$)	294	Relative humidity imposed using 6 mL of 3.25 wt% NaCl solution with **40% enrichment of $H_2{}^{17}O$**[c]	**Relative humidity**	Solid state NMR of glass powder[d]	213
	6		Monolith ($2.5 \times 2.5 \times 0.1$ cm)	1384		98%	SEM, XRD, ToF-SIMS	213
	7	QCa	Powder ($0.45 < \Phi < 2\,\mu m$)	294			Solid state NMR of glass powder[d]	
	8		Monolith ($2.5 \times 2.5 \times 0.1$ cm)	2052			SEM, XRD, ToF-SIMS	

[a]All experiments were carried out at 90 °C.
[b]The glass surface area of the powder samples were measured using BET. Surface area of glass Q is 5 $m^2\,g^{-1}$ and that of the glass QCa is 4.64 $m^2\,g^{-1}$. The glass surface area of the polished monolith samples were calculated from the sample dimensions.
[c]The DI water with 40% enrichment of $H_2{}^{17}O$ is also enriched in ^{18}O.
[d]For the solid state NMR spectroscopy of the glass powders, the following spectra were acquired: ^{11}B MAS, $^{11}B\{^1H\}$ REDOR, ^{17}O MAS, ^{17}O MQMAS, ^{23}Na MAS, ^{23}Na CPMAS, $^{23}Na\{^1H\}$ REDOR, ^{27}Al MAS, ^{27}Al CPMAS, $^{27}Al\{^1H\}$ REDOR, ^{29}Si MAS, ^{29}Si CPMAS. The NMR spectra from experiment 1 are called as Q-AM, experiment 3 as QCa-AM, experiment 5 as Q-VP, and experiment 7 as QCa-VP.
Bold characters are used to draw attention of the reader to the samples altered in oxygen-17 entriched water.

conducted with the glass QCa. Experiments 5 and 6 were carried out in a single reactor and experiments 7 and 8 were similarly carried out in another single reactor.

RESULTS

Alteration kinetics

Glass alteration in both media resulted in the formation of an altered or gel layer on the glass surface. This section provides information on the altered glass percentage and altered layer thicknesses for each glass. It also gives information on the effect of Ca on glass alteration kinetics in aqueous medium and vapor phase.

Aqueous alteration. Figure 1 shows the evolutions of pH and the altered glass percentage for the glasses Q and QCa (experiments 1–4).

The average $pH_{90°C}$ of the leachate of the glass Q in experiment 2 was 9.2 (±0.2). There was no pH evolution with time starting from the very first sampling done after 7 days of leaching. SE images of the altered glass powders at the end of the experiment did not show the presence of any secondary precipitates (Supplementary Fig. 1). The pH value is consistent with other aqueous alteration experiments conducted at a very high SA/V ratio[18].

The average $pH_{90°C}$ of the QCa-leachate in experiment n°4 was 9.6 (±0.2). The pH value remained stable throughout the experimental duration. XRD analysis of the QCa glass powders (experiment 4) after aqueous alteration indicated the formation of calcite (Supplementary Fig. 2).

According to the evolution of the altered glass percentage of glass Q shown in Fig. 1, almost 86% of the glasses were altered within 28 days for the experiment 2 and it was expected that

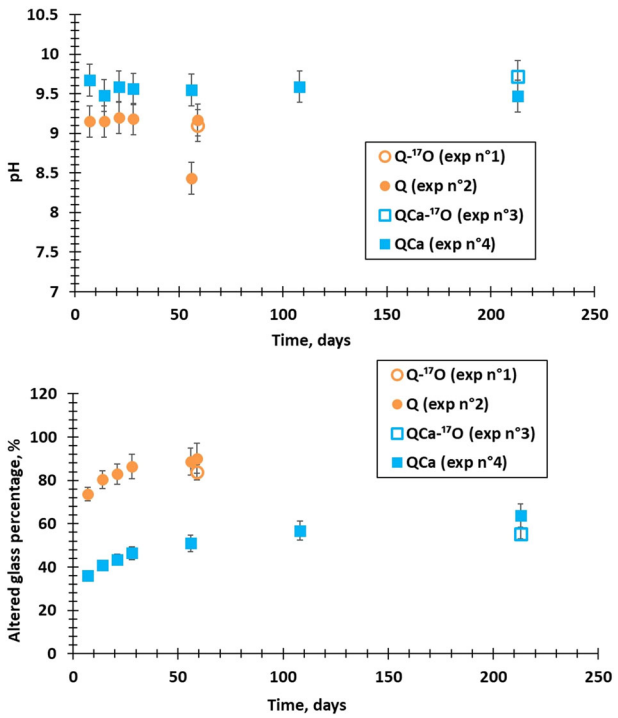

Fig. 1 pH and altered glass percentages time evolution. Solution analysis results for the aqueous alteration experiments 1, 2, 3 and 4 in Table 1: (top) Evolution of pH with time (fixed error of ±0.2 based on measurement device); (bottom) evolution of percent of altered glass with time (error calculated from the propagation of the error values associated with the boron concentration measured using ICP-OES).

experiment 1 would also follow a similar evolution. The $pH_{90°C}$ measurement on the 56th day showed a decrease from 9.2 to 8.4. Since there was concern that this decrease might be due to zeolite precipitation, which in turn might deteriorate the gel layer, this experiment was stopped after 59 days of aqueous alteration. It was judged that 86% of alteration was sufficient to study the gel layers using NMR spectroscopy. The alteration of the QCa glass on the other hand was comparatively slower with only 46% alteration after 28 days. Therefore, the alteration was continued until 213 days, after which around 64% of the glass had altered. This comparison of the altered glass percentage of the Q and QCa glasses clearly shows the positive effect of the incorporation of Ca in the glass on the glass chemical durability. This is in contrast to Ca effect in vapor phase and this will be addressed further.

Vapor phase alteration

SEM images: Glass Q: SEM images help to physically distinguish the altered layer morphology due to density differences between the pristine glass and the gel layer. A portion of the altered monoliths from experiments 6 and 8 in Table 1 were enrobed in epoxy resin, polished to an optical surface finish, and observed in BSE for cross-section images (see Fig. 2a). According to this image, the glass Q has a clearly distinguishable altered layer of approximately 1 µm thickness. The gel layer seems homogeneous and appears fractured and detached intermittently. Direct observation of the altered surface (Fig. 2c) indicates the presence of some scattered unidentified secondary phases. XRD pattern shows the presence of a small peak that could correspond to kaolinite (Supplementary Fig. 3). Kaolinite is often identified on naturally weathered/hydrothermally altered basaltic volcanic glass[36], although its effect on glass alteration kinetics is not well known.

Glass QCa: According to the cross-section BSE image in Fig. 2b, the altered layer in the glass QCa seems to be around 1.7 µm thick approximately, although the contrast between the gel layer and the pristine glass seems to be very low. The gel layer appears homogeneous. The direct observation of the altered surface (Fig. 2d) shows some scattered unidentified precipitates. The XRD pattern did not contain any peaks (Supplementary Fig. 3). According to the SEM results, it seems that the glass QCa has altered more than the glass Q for the same duration in vapor phase. This could suggest a slightly negative effect of Ca in vapor phase at 90 °C. In previous work, the glass QCa altered slightly faster than the glass Q in vapor phase at 50 °C too[27].

ToF-SIMS: Figure 3 shows the normalized ToF-SIMS profiles of the monolith samples altered in experiments 6 and 8. Using these profiles, the altered layer depth and the depth of penetration of hydrogen and ^{17}O ions into the gel layer were calculated to be 277, 308, and 269 nm, respectively, for the glass Q and 285, 341, and 284 nm, respectively, for the glass QCa. Surprisingly, the gel layer thickness measured using ToF-SIMS does not correspond with the thickness measured through SEM images. In literature, a good correspondence between gel layer thickness measured between SEM and ToF-SIMS has been frequently reported[27,29–31], which makes the discrepancy in our study enigmatic. The following hypothesis could be considered, although it is not verifiable for these samples. During ToF-SIMS analysis, the same speed of abrasion was used for the entire sample (secondary phases, gel, and pristine glass). If the gel layer were abraded at a much quicker rate than the pristine glass due to a lower density, this could result in an underestimation of the gel layer thickness. In another study on the vapor hydration of SON68 nuclear waste glass simulant, it was shown that the altered layer thickness could be underestimated by a factor of up to 4 from ToF-SIMS measurements[32]. Based on the ToF-SIMS results, it could be said that the addition of Ca in the QCa glass has an almost negligible effect on the vapor hydration rate.

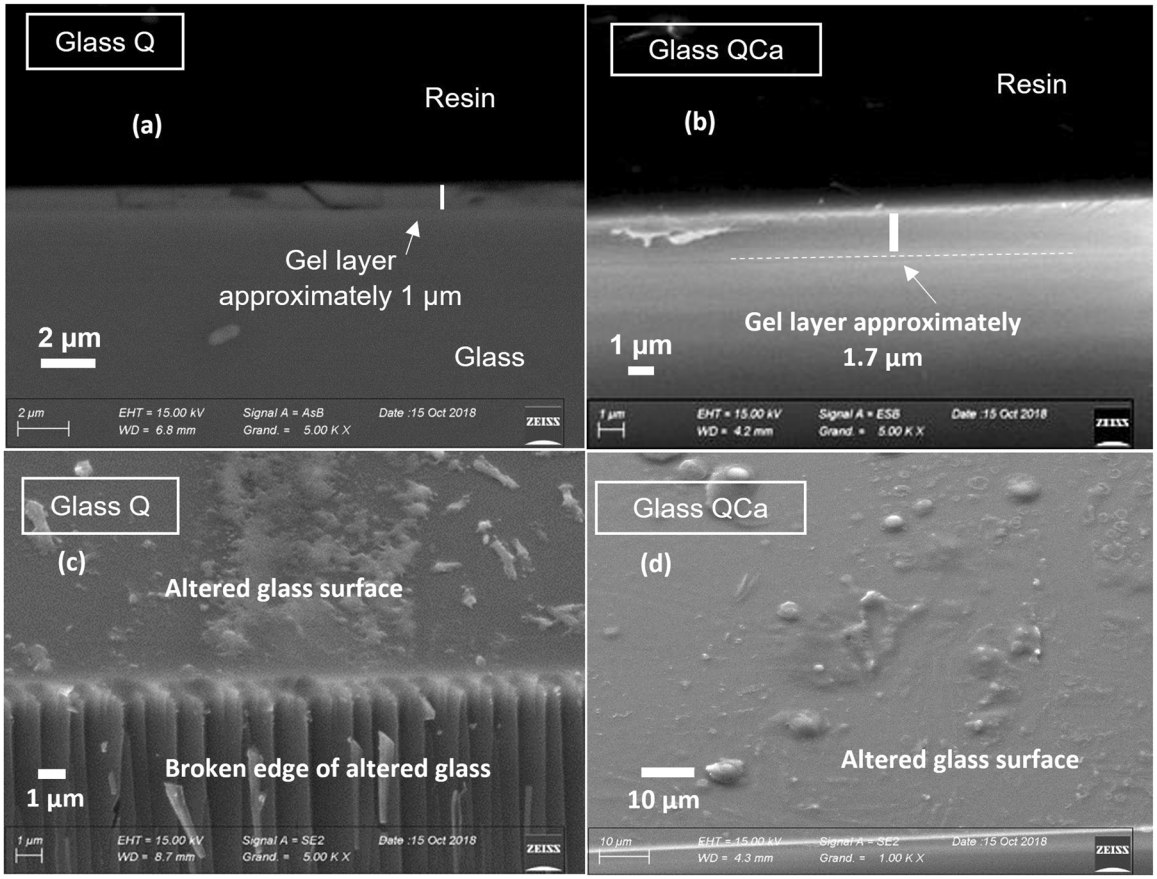

Fig. 2 SEM images of glasses altered in vapor phase. SEM images of Q (left) and QCa (right) glass altered in vapor phase (experiment no. 6 and 8, respectively, in Table 1); **a** cross-section BSE image of vapor-hydrated glass Q; **b** cross-section BSE image of vapor-hydrated glass QCa; **c** SE image of direct observation of vapor-hydrated glass Q surface; **d** SE Image of direct observation of vapor-hydrated QCa glass surface.

Behavior of elements in the gel layer

Vapor phase alteration. The ToF-SIMS profiles shown in Fig. 3 also describe the behavior of elements in the gel layer. The H intensity peaks is slightly higher than the SiOH intensity at the gel surface and the gel-glass interface. The profiles of ^{17}O and ^{18}O, sourced from the saline solution used to control the vapor phase, are uniformly enriched in the gel layer region, and do not show peaks at the surface or the gel-glass interface, unlike the H profiles. These profiles suggest that the gel layer is quite homogeneous in nature.

In both glasses, boron is the most depleted element in the gel layer. Its average retention factor in the gel layer is only around 9% for the Q glass and around 13% for the QCa glass (based on Fig. 3a, b). The ToF-SIMS normalized profiles indicate that there might only be a slight depletion of Al and Na in the gel layer for both glasses. The surface of both Q and QCa glasses showed some scattered secondary phase precipitation. This could perhaps explain this loss. Na slightly peaks at the gel-glass interface like the H profile.

By closely observing the ToF-SIMS profiles in our previous studies, a similar combined enrichment of Na^+ and H^+ has been observed in some cases[27,31,37].

In case of the QCa glass, there is a significant depletion of Ca in addition to that of boron. Additionally, there is an increasing trend in Ca-concentration towards the surface of the gel layer. This could be related to the formation of Ca-containing secondary phases. Although, XRD patterns on monoliths did not indicate the formation of any phases. It is possible that the quantity of phases was insufficient, or the phases were poorly crystalline.

The gel-glass interface thickness of the QCa glass as defined by the profiles of H and O (≈100 nm) seems to be much wider than that of the Q glass (≈60 nm) (from Fig. 3). The gel-glass interface thickness of the QCa glass as defined by the boron profile (≈60 nm) is also larger than that of the Q glass (≈30 nm). The difference in the interfacial thicknesses that were determined by the boron profiles and that of the H, SiOH and O profiles suggest that in both glasses, there exists a hydrated layer without any element loss between the pristine glass and gel layer.

Aqueous alteration. The Normalized mass Losses of elements (NL) with time for the glasses Q and QCa are given in Supplementary Table 1. The NL values of boron are the highest. The high solubility of boron during aqueous alteration of glasses and its negligible retention in the gel layer is quite well known in the field and it is for this reason that it is used as a glass alteration tracer[38]. The nominal composition of elements in the gel layer (excluding boron, hydrogen, and oxygen) at the end of the experiment can be calculated using the relation Retention factor $RF_i = 1 - \frac{NL(i)}{NL(B)}$. The calculated RF_i values and the gel layer composition are provided in Table 2. The relative retention of Si and Al in the gel layer is almost 100%. In pristine glass, we can assume that all the Al is in 4-coordinated state i.e. $[AlO_4]^-$. Na^+ ions play the role of charge compensator for these $[AlO_4]^-$ units[6,20,39]. From the pristine glass composition, it can be seen that there is an excess quantity of Na than Al in the glass (for both Q and QCa). Na also plays the role of charge compensators for four-coordinated boron (BO_4) units. The remaining Na is present as network modifiers in the glass next to non-bridging

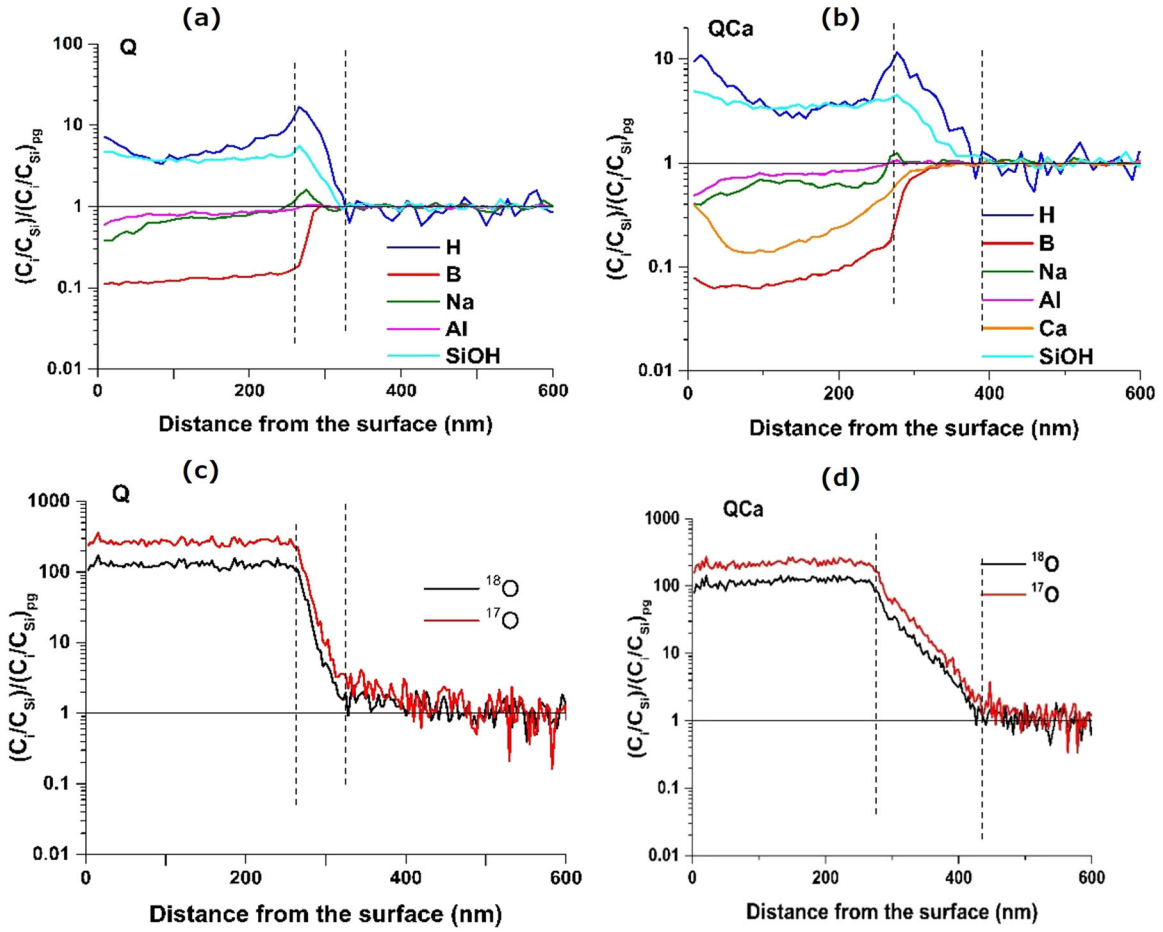

Fig. 3 ToF-SIMS. Normalized ToF-SIMS profiles of glass Q and glass QCa monoliths altered in vapor phase (experiments 6 (**a**, **c**) and 8 (**b**, **d**)).

oxygen atoms. In the gel however, Na retention is only around 48% for the Q glass and 33–36% for the QCa glass. Looking at the gel layer composition, the at. mol% of Na is quite close to that of Al for both glasses. This suggests that the Na that were present as network modifier in the glass and most of the Na that played the role of charge compensator to BO_4 units have been leached out and only the Na^+ ions which played the role of charge compensator to $[AlO_4]^-$ have been retained in the gel layer. Such an interpretation assumes that the Al is present in the 4-coordination state in the gel layer too. The retention of Ca in the gel layer is approximately 98% in the QCa glass, which is much higher than in QCa altered in vapor phase. The retention of Ca in the gel layer has a passivating effect[3,33,40,41]. According to Table 2, at least a small portion of Ca^{2+} must be playing the role of charge compensation for $[AlO_4]^-$ units. This Al-Ca synergy effect in the gel layer is well-known for its passivating properties. XRD identified the presence of calcite in the altered glass powders. One of the mechanisms by which Ca in the gel layer may be passivating is by precipitation in the pore water of the gel layer, which slows down water diffusion through the gel layer[40]. Despite secondary phase precipitation, QCa can be considered to have a passivating gel layer, since the precipitate that formed is calcite and not calcium-silicate-hydrates (CSHs) that could have an antagonistic effect[34].

Structure of the gel layer

In this section, the NMR spectroscopy results are presented to study the structural evolution of the glass network as a result of alteration in aqueous medium (denoted AM) and vapor phase (denoted VP). In the case of experiments 5 and 7, i.e., Q and QCa glass powders altered in vapor phase, a peculiar behavior of the glass powders was observed. When the vapor phase reactors were opened at the end of the experiment, liquid water appeared to have condensed on top of the powders. It is unknown if this water condensation occurred over the course of the duration of the experiment as a result of capillary condensation on the powders or if it occurred at the end of the experiment while the reactor was cooled to room temperature before being opened. In any case, the comparison between the two different methods of alteration still remains interesting. Based on the objective of the study and to easily distinguish between the experiments, the glass powders altered in experiments 5 and 7 are still referred to as vapor phase or VP samples. The powder samples were dried overnight at 90 °C before NMR spectroscopy was performed.

^{17}O NMR. The ^{17}O MAS NMR spectra of pristine Q and QCa glasses were recorded on approximately 200 mg ^{17}O enriched pristine glasses (denoted as pg-^{17}O) of the same composition prepared via sol-gel synthesis method. Supplementary Figs. 4 and 5 show MAS NMR spectra of ^{11}B, ^{23}Na, ^{27}Al and ^{29}Si nuclei in the pristine non-enriched glass (denoted as pg) and in the pg-^{17}O. These data confirms that the structure of the two pristine glasses of the same theoretical composition, but using different synthesis routes and ^{17}O isotopic abundance, have a very close structure (in terms of the speciation of the probed elements). Therefore, the ^{17}O spectra of the gel layer formed on the unenriched glasses can be compared with the environment of ^{17}O in the enriched pristine glasses.

Figure 4 shows the ^{17}O MQMAS NMR spectra. Q-AM shows clear evidence for the recondensation of Si and Al with ^{17}O from the

Table 2. Calculated retention factor of elements in the gel layer at the end of the experiment for the aqueous alteration experiments and composition of gel layer and pristine glass (excluding boron, oxygen and hydrogen).

	RF_i				At mol% in pristine glass (excluding B, H, and O)		At mol% in gel (excluding B, H, and O)	
	Exp. 1 (Q)	Exp. 2 (Q)	Exp. 3 (QCa)	Exp. 4 (QCa)	Q	QCa	Q	QCa
Si	0.994	0.995	0.989	0.989	51.34	47.07	62.33	60.82
Al	1.000	1.000	1.000	0.998	14.41	13.39	17.59	17.49
Na	0.480	0.479	0.327	0.359	34.25	33.97	20.08	14.52
Ca			0.985	0.976		5.57		7.17

aqueous medium. But there is no evidence for boron recondensation with ^{17}O. For the samples Q-VP and QCa-VP, there is clear evidence for boron recondensation in the gel layer with ^{17}O coming from the vapor phase, along with the expected Si and Al recondensation in the gel layer. Additionally, there is also evidence of ^{17}O recondensation with Na as Si-^{17}O-Na only in the QCa-VP sample. ^{17}O does not recondense with Ca in the QCa-VP sample. In the Q-VP sample, ^{17}O does not recondense with Na. The 2D MQMAS spectrum of QCa-AM is unfortunately too noisy to draw clear conclusions. This may be because of the weaker alteration of the QCa-AM sample (55.3 ± 2.3%) relative to the other samples.

Figure 5 shows the ^{17}O MAS NMR spectra. Differences are observed in the 50–100 ppm region, notably for the Q-VP samples. Only the pristine and vapor phase altered samples (Q-VP and QCa-VP) have a contribution in the 50–100 ppm range (attributed to B-^{17}O-B species, according to the MQMAS spectra shown in Fig. 4), whereas the Q-AM and QCa-AM do not show any signal in this region. Figure 5c, d show the isotropic projection of the MQMAS spectra (that is the dimension free of second order quadrupolar broadening seen in the MAS dimension). These spectra confirm that the additional contribution around 50–100 ppm in the ^{17}O MAS dimension is mainly due to the presence of B-^{17}O-X species in both the pristine and altered samples[42].

It can be noticed from Fig. 5c that in the glass Q, the ratio of Si-^{17}O-Si and Si-^{17}O-Al proportions is similar in the pristine glass and the gel formed in aqueous medium. In the gel formed in vapor phase, the proportion of Si-^{17}O-Si is much higher than Si-^{17}O-Al. In contrast, Fig. 5d shows that the proportion of Si-^{17}O-Al is very high in the QCa-VP sample than the Si-^{17}O-Si. Also, in the pristine glass of both Q and QCa, the Si-^{17}O-B proportion is higher than the B-^{17}O-B species. However, in the altered Q-VP and QCa-VP samples, the proportions of both Si-^{17}O-B and B-^{17}O-B are similar (according to Figs. 4c, f and 5c, d). The signal to noise ratio in the QCa-AM sample is very poor in the Figs. 4e and 5d to draw meaningful conclusions.

^{29}Si, ^{27}Al, and ^{23}Na NMR. Figure 6a, b show the ^{29}Si MAS NMR spectra for the Q and QCa glasses. The ^{29}Si MAS signal of the QCa-VP sample clearly shows four resolved peaks at −93, −98, −104 and −110 ppm, which correspond to $Q^1Si(3Al)$, $Q^2Si(2Al)$, $Q^3Si(1Al)$ and $Q^4Si(0Al)$ structures of NaY-zeolites[43] These signals coming from the zeolites can be filtered out using CPMAS as shown in Fig. 6c suggesting that the zeolites were dehydrated by the 90 °C heating before NMR characterization. There is much less difference in the CPMAS spectra as it probes mainly the protonated zone in the alteration layer. The crystallinity of the zeolites were probably poor since the XRD pattern did not indicate their presence.

The ^{27}Al MAS NMR spectra shown in Fig. 6d–f show that Al is exclusively in 4-fold coordination state[44]. In the altered Q and QCa samples, a narrower ^{IV}Al signal is detected. Such a narrowing has been already observed in the ^{27}Al MAS spectra of glass alteration gels[6,45] and is usually associated with the presence of water molecules in Al surroundings[46], which reduce the local electric field gradient and thus the induced quadrupolar broadening. VP and AM samples show similar ^{27}Al MAS NMR spectra, except for the gel layer formed on the QCa sample altered in vapor phase (QCa-VP) which has a narrower peak than the other three gels and also shows a slightly more positive shift. The peak position (≈60 ppm) also indicates that there is a contribution from zeolites[43]. The ^{27}Al CPMAS NMR experiment suppresses the signal contribution from the zeolites (as in ^{29}Si experiments, thus corroborating the dehydration of the zeolite) and the CPMAS spectra of the QCa-VP sample shown in Fig. 6f resembles that of the other three samples. These results seem to confirm the precipitation of zeolites in the QCa powder sample altered in vapor phase.

The ^{23}Na MAS spectra shown in Fig. 6g, i of the altered samples exhibit narrowing of the peaks at a similar peak position, with a more positive chemical shift, compared to the unaltered samples. This reduction in linewidth and positive chemical shift is associated with an increase in hydration of the samples[44]. However, in the ^{23}Na CPMAS NMR spectra in Fig. 6h, j, similar line shapes are observed for all samples and the narrower components of the ^{23}Na MAS spectra (for the samples Q-AM and QCa-VP) are strongly attenuated. Only in the QCa-VP sample, the MAS spectra shows a small contribution around δ_{iso} 4.5–5 ppm next to the distinctive sharp peak at around δ_{iso} −6.5 ppm. This suggests that some of the Na^+ ions are in a slightly different environment than the rest since δ_{iso} is sensitive to Na-O bond distance and coordination of the Na^+ ions. The NMR spectra associated with NaY-zeolites in the literature seem to vary depending on a number of parameters[47,48]. Therefore, it is difficult to attribute any peak positions or characteristics observed in this study to that of the NaY-zeolites for the ^{23}Na NMR spectra. These narrow peaks are more likely to result from more hydrated Na species enabling a higher mobility, thus inducing a motional narrowing mechanism. This mobility can result in a loss of efficiency of the cross-polarization (CP) magnetization transfer from ^1H to ^{23}Na, thus explaining the observed differences in CPMAS.

^{11}B NMR. Figure 7 shows the experimental and simulated ^{11}B MAS NMR spectra of the pristine and altered samples. The chemical shift of BO_4 lines is more positive in the altered samples by about 0.8–1.3 ppm when compared to that of the pristine samples. This shift could be linked to a change in the first and second neighbors of boron atoms. It can also be observed that the altered samples have a higher fraction of BO_4 than in the pristine glasses. This suggests that BO_3 units are more soluble than BO_4 units and are therefore leached more rapidly as was already observed in literature for alteration of borosilicate glasses in aqueous medium[38,49]. This is true for vapor hydration of borosilicate glasses as well since recent finding suggested that the loss of boron from the gel layer is most likely in the form of B-$(OH)_3$ species[50] that can be volatile at higher temperatures and concentrations[51]. Although, unlike ref. [50], there is no clear evidence of transformation of 4-coordinated BO_4 units to

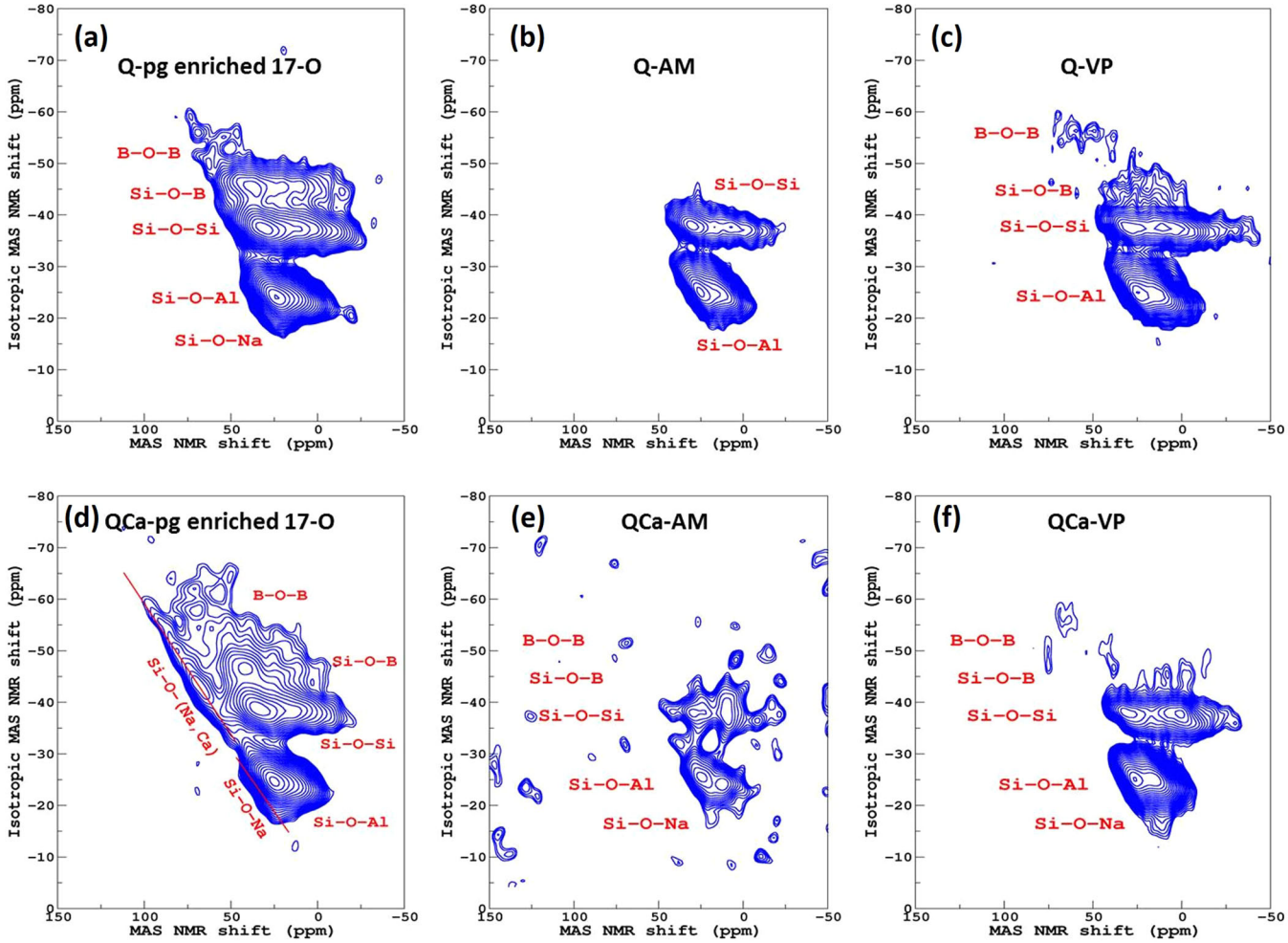

Fig. 4 ^{17}O MQMAS NMR spectra. a pristine Q glass enriched in ^{17}O (Q-pg enriched 17-O); **b** unenriched Q glass altered in ^{17}O-enriched aqueous medium (Q-AM); **c** unenriched Q glass altered in ^{17}O-enriched vapor phase (Q-VP); **d** pristine QCa glass enriched in ^{17}O (QCa-pg enriched 17-O); **e** unenriched QCa glass altered in ^{17}O-enriched aqueous medium (QCa-AM); **f** unenriched QCa glass altered in ^{17}O-enriched vapor phase (QCa-VP).

3-coordinated BO_3 units. It is possible that the evidence might be masked due to the possibly faster dissolution rate of the BO_3 units than the transformation rate of the BO_4 units.

X-{^{1}H} Rotational Echo DOuble Resonance (REDOR) experiments. Since samples may not have been altered to the core, the NMR signals in the altered samples are the superposition of the signals from the residual pristine glass and the gel layer. In order to clarify this, REDOR experiments were carried out on all four altered samples. These experiments were found to be more robust and sensitive than CPMAS experiments. These experiments allow us to quantify the fraction of B, Al or Na in the sample that is in close proximity to protons, and thus can be considered as part of the altered sample or gel layer. Its principle is to collect first a (reference) spin echo decay $S_0(t)$ on ^{11}B, ^{27}Al or ^{23}Na and then, in a second experiment, the echo decay $S(t)$ while irradiating ^{1}H with a rotor-synchronized train of 180° pulses, which aims at reintroducing the (^{11}B/^{27}Al/^{23}Na)-^{1}H (magnetic) dipolar interactions. This causes an additional decrease of the echo intensity that is controlled by (^{11}B/^{27}Al/^{23}Na)-^{1}H proximities. The part of the echo decay that is only due to (^{11}B/^{27}Al/^{23}Na)-^{1}H dipolar interactions can then be extracted from a normalized difference signal denoted as $\Delta S(t)=\{S_0(t)-S(t)\}/S_0(t)$. Thus, the renormalized REDOR signal $\Delta S(t)$ approaches 1 if all the ^{11}B/^{27}Al/^{23}Na nuclei are (dipolar)-coupled to the ^{1}H. Note that selective pulses on the ^{11}B/^{27}Al/^{23}Na central transition are applied so that contribution of the satellite transitions can be ignored (and indeed, no spinning sidebands are observed in the data). Once the REDOR curve is plateauing, it can be considered that the residual signal is due to un-coupled nuclei, that is non-hydrated B/Al/Na species (i.e., in the residual core glass) in our case. This is confirmed by the images shown in Supplementary Fig. 6 showing that the REDOR filtered MAS spectrum is close in shape (not in intensity because of the echo filtering) to the MAS NMR spectrum of the glass. According to the $\Delta S(t)$ REDOR curves shown in Fig. 8, the hydrated fraction of species in the altered samples is as follows: ≈70% of ^{11}B, ^{27}Al and ^{23}Na in the Q-AM sample, ≈65% ^{11}B and ≈60% ^{27}Al and ^{23}Na in the QCa-AM sample, ≈80% ^{11}B and ^{23}Na and ≈70% ^{27}Al in Q-VP sample and ≈85% ^{11}B and ≈80% ^{23}Na and ^{27}Al in the QCa-VP sample. See Supplementary Figs. 7–9 for $S_0(t)$ and $S(t)$ curves for ^{11}B{^{1}H}, ^{27}Al{^{1}H}, and ^{23}Na{^{1}H}, respectively.

DISCUSSION

The following paragraphs discuss the inferences about glass alteration mechanisms that can be drawn from the alteration kinetics results

In aqueous medium, the glass Q has altered faster than the glass QCa. The role played by Ca on glass alteration kinetics across a range of pH and SA/V ratio is well documented in the

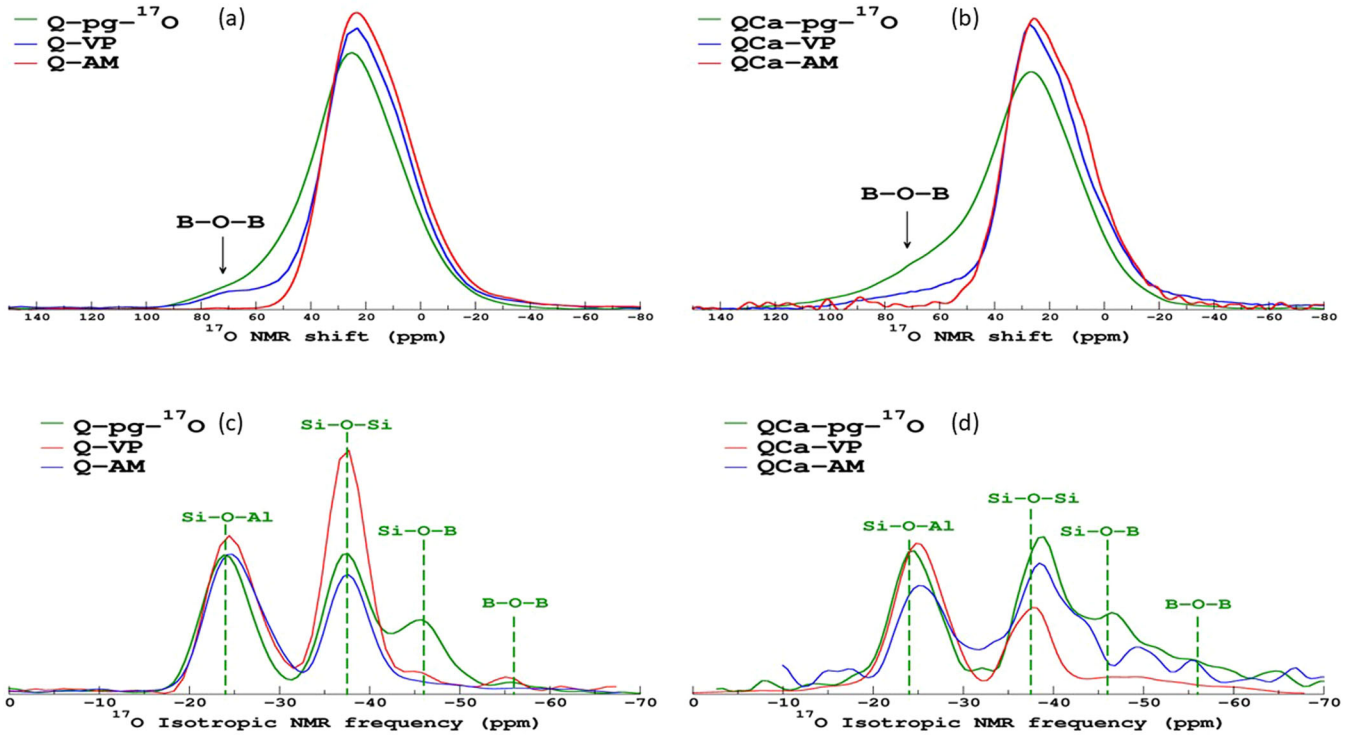

Fig. 5 ^{17}O MAS NMR spectra. **a**, **b** The pristine samples enriched in ^{17}O (called pg-^{17}O), samples altered in aqueous medium (called AM) and samples altered in vapor phase (called VP) of the **a** Q glass and the **b** QCa glass; **c**, **d** projections in the isotropic dimension of the ^{17}O MQMAS NMR spectra for the Q and the QCa samples respectively (pristine, altered in vapor phase and in aqueous medium).

literature[34,40,41]. In this case, the value of pH is not high enough to trigger the precipitation of Calcium-Silicate-Hydrates (CSHs) or zeolites, which may increase the glass alteration rate[52]. The SA/V ratio is high enough to quickly form a gel layer with good Ca-retention that has a strong passivating effect and has reduced the glass alteration rate[33,41,53]. Therefore, the slower alteration of the glass QCa can be attributed to the effect of Ca, which is positive under the given conditions. Based on the evolution of the altered glass percentage in Fig. 1 and its comparison to standard glass alteration profiles available in the literature[3,53], it can be said that the glass alteration with time evolved with different mechanisms being rate-controlling at different times. Inter-diffusion, network-hydrolysis, gel layer formation by condensation/precipitation of Si, Al, Ca and water diffusion through the gel layer successively must have been the rate-controlling mechanisms of glass alteration. However, the slower alteration of the glass QCa relative to the glass Q suggests that the glass alteration rate was rather predominantly controlled by the water diffusion rate through the gel layer. This also indicates that the gel layer was formed before the first sampling of the aqueous solution conducted at 7 days after the start of the experiment. The NMR results show evidence of hydrolysis followed by condensation/precipitation of Si and Al in the gel layer with ^{17}O coming from the aqueous medium.

In vapor phase, the alteration rates of glass Q and glass QCa are almost similar, with the glass QCa having a slightly higher alteration rate. This may be due to two possible reasons. The first one is that there might be a negative effect of Ca, as it can be supposed that the pH of the system must be highly basic and at significant reaction progress, CSHs or zeolites may be beginning to precipitate. It has been shown that the precipitation of zeolites could increase the alteration rate by destabilizing the gel layer due to Si, Al, Na and Ca losses[52,54]. This hypothesis could be supported by the fact that the NMR signal of the QCa-VP suggested the presence of zeolites. The NMR was carried out on glass powders. The XRD pattern of the monolith sample of QCa did not suggest the presence of any secondary phases, although SE image of the glass surface (Fig. 2(d)) indicated the presence of some unidentified secondary phases. Despite the evidence for the precipitation of secondary phases in the QCa glass, it is not clear if it acts a driving force for the higher glass alteration or is merely a consequence of glass alteration without any impact on the rate.

The other possible reason for the slightly higher alteration of the glass QCa is that the glass QCa is less polymerized than the glass Q. The NBO fraction of the pristine glass Q is 0.036, whereas for the glass QCa it is 0.111[27]. If network hydrolysis was one of the predominant rate-controlling glass alteration mechanisms in vapor phase, and if the QCa gel layer was not passivating with Al-Ca synergy, this would explain the slightly higher alteration of the QCa glass. In vapor phase, there is clear evidence for the hydrolysis and condensation/precipitation of Si, Al, Na and even B with ^{17}O supplied by the vapor phase. However, it is not clear if hydrolysis acted as a rate-controlling mechanism.

For aqueous medium, the alteration kinetics was followed periodically through regular sampling of solution and therefore an evolution of the altered glass percentage with time was established. However, in vapor phase, the extent of glass alteration for the Q and QCa glasses were simply compared at the end of the experiment. Therefore, a direct comparison of the evolution of the rate-controlling mechanisms over time between glass alteration in aqueous medium and vapor phase cannot be made. It is possible that unlike aqueous medium, network-hydrolysis was the predominant rate-controlling mechanism in vapor phase. It is also possible that the alteration rate evolution in vapor phase followed a similar path to alteration rate in aqueous medium with Ca-retention in the gel layer in synergy with Al, but zeolites precipitation resulted in a state of "alteration resumption"[52] for the glass QCa towards the end and ultimately ended-up being the more altered glass.

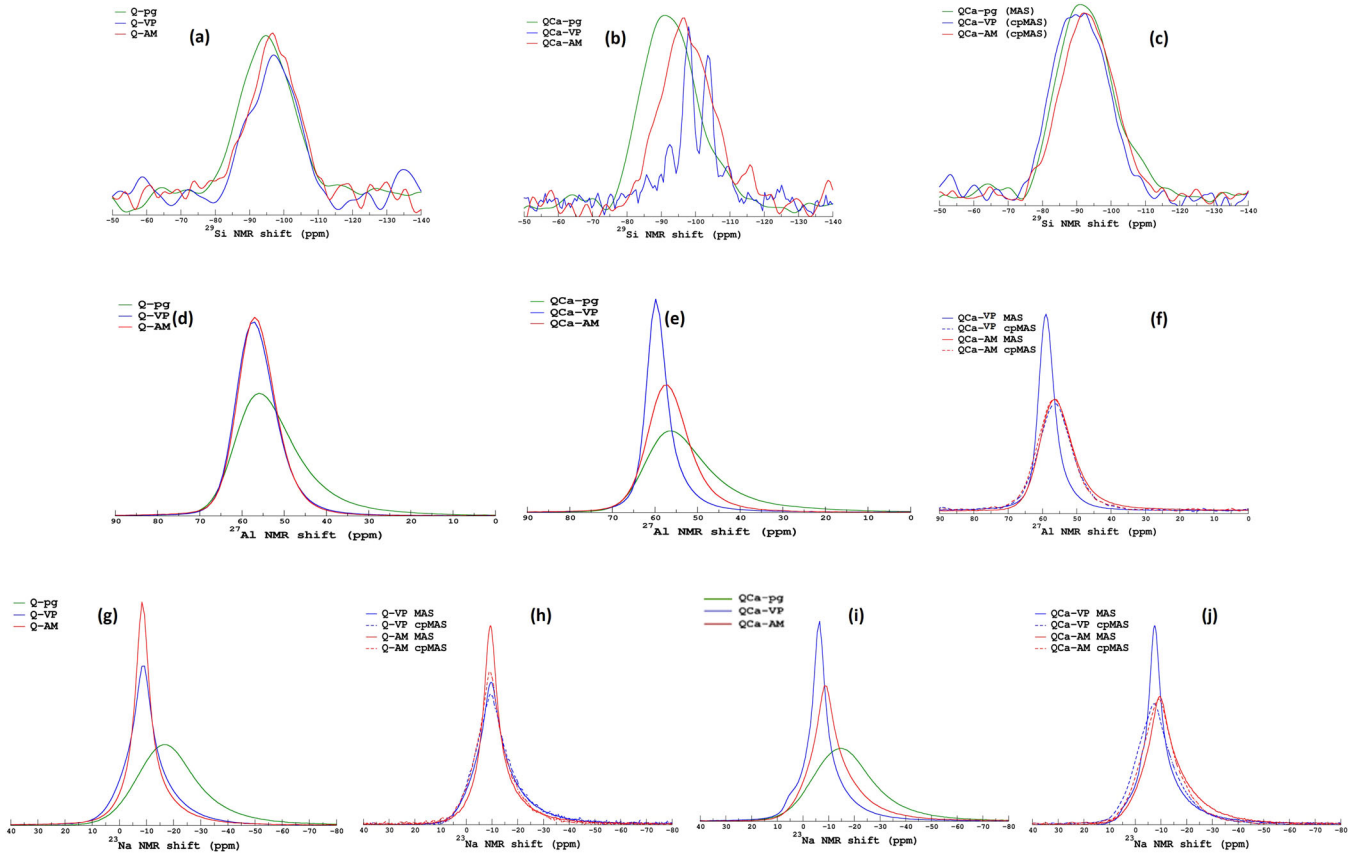

Fig. 6 ^{29}Si, ^{27}Al and ^{23}Na MAS and CPMAS NMR spectra. a, **b** ^{29}Si MAS NMR spectra of the unaltered (pristine) glass of natural isotopic abundance (pg), glass altered in vapor phase (VP) and aqueous medium (AM) for the Q and QCa glass respectively; **c** ^{29}Si CPMAS spectra for QCa glass altered in vapor phase (VP) and aqueous medium (AM) and ^{29}Si MAS NMR spectra of the unaltered pg sample; **d**, **e** ^{27}Al MAS NMR spectra of pg, VP and AM samples of Q and QCa glasses respectively; **f** ^{27}Al MAS and CPMAS NMR spectra for AM and VP samples of QCa glass; **g** ^{23}Na MAS NMR spectra of pg, VP and AM samples of the Q glass; **h** ^{23}Na MAS and CPMAS NMR spectra for AM and VP samples of the Q glass; **i** ^{23}Na MAS NMR spectra of pg, VP and AM samples of the QCa glass; **j** ^{23}Na MAS and CPMAS NMR spectra for AM and VP samples of the QCa glass.

The significant results from the study of behavior of elements in the gel layer are discussed in the below paragraphs

In aqueous medium, information on the behavior of elements in the gel layer was mostly extrapolated from the measurement of concentration of glass species in the alteration solution in the form of retention of elements in the gel layer (given in Table 2). Table 2 assumes that there is no boron retention in the gel layer even though the ^{11}B{^{1}H} NMR REDOR of the Q-AM and the QCa-AM suggest the presence of boron in the proximity of ^{1}H. It is known that there could be boron retention in the gel layer close to the interface and the retention of boron increases as a gradient towards the pristine glass[11,14,38]. The thickness of this interface with a gradient boron retention could be up to a few tens of nm. In a powder sample with such a small particle size and numerous grains, which have not been altered to the core, it is not surprising that there is enough boron in the numerous interfaces to generate a signal for the ^{11}B{^{1}H} NMR REDOR experiments (and in CPMAS experiments, see supplementary information). It is still valid to assume that in a gel layer formed in aqueous medium, boron retention is negligible as it is one of the most soluble elements in the glass and remains the best tracer for calculation of glass alteration rate[11,38].

For the monolith samples altered in vapor phase, the ToF-SIMS profiles provide direct insights into the behavior of elements in the gel layer. The ToF-SIMS profiles portray clearly distinguishable three zones: the pristine glass, an interface, and a gel layer. Firstly, it is noticeable that the interface of the QCa glass is wider than the interface of the Q glass. This could be because the hydrated radius of a divalent cation is larger than that of a monovalent cation. The presence of hydrated Ca^{2+} ions in the interface might be the reason behind the larger interface for the Ca-containing glass. Next, for both glasses, the interfacial thickness marked by H, SiOH and ^{17,18}O is larger than that marked by the boron profile. This suggests the presence of 2 zones within the interface: a layer close to the pristine glass that is hydrated without loss of elements, followed by a zone where the element loss begins.

The H and ^{17,18}O profile shapes are similar in the interface. This suggests that in the interface, H_2O molecules may be predominantly present, suggesting penetration of water molecules. In the gel layer, the H and ^{17,18}O profile shapes are dissimilar. The water molecules might have dissociated to form silanol and Na-OH groups. Therefore, the H and ^{17,18}O profile shapes in the gel layer might be more influenced by the glass species they are associated with. ^{17}O recondensed with Si, Al and B in the gel layer according to NMR results. The profile shapes of these elements in the gel layer, including that of SiOH, are straight and similar to that of ^{17}O.

The H profile shape seems to be more closely associated with the Na profile. The H^+ and Na^+ ions might engage in ion-exchange reactions but may remain fairly close to each other and result in ToF-SIMS profile shapes that are quite similar. Both Na and H profiles peak at the interface. Perhaps this could be explained based on the Molecular Dynamics study carried out by Jabraoui et al. on the glass-water interface[55]. During the initial interaction between glass and water molecules, there is a high

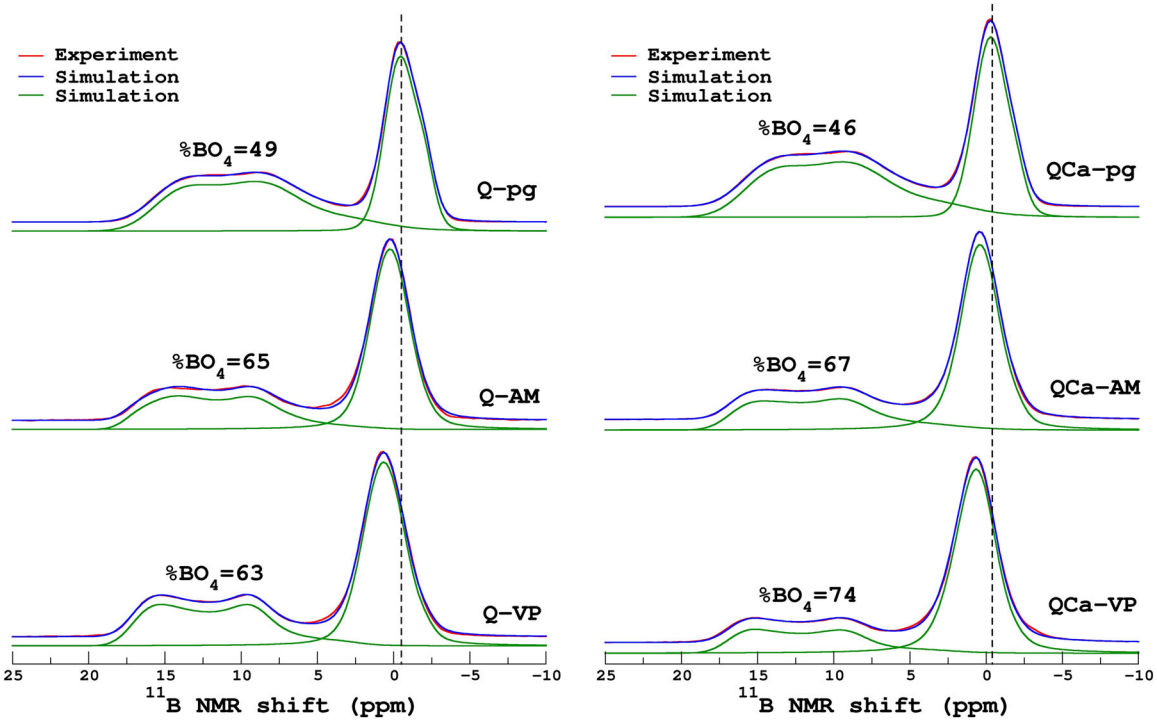

Fig. 7 ^{11}B MAS NMR spectra. Experimental and simulated ^{11}B MAS NMR spectra of pg, AM and VP samples; (left column) Q glass and (right column) QCa glass. The spectra have been simulated as described in refs. [15,65]. Four (pg) components have been fitted using the pristine glass ($2 \times BO_3$ and $2 \times BO_4$). While keeping the pg NMR parameters constant, two components have been fitted for the altered glasses ($1 \times BO_3$ and $1 \times BO_4$). For altered glasses, the residual glass contribution was found to be around 10 (±5)%.

affinity between Na^+ and water molecules. Therefore, while water molecules penetrate the glass network, partially adsorbed water molecules may surround Na^+. This might reduce the mobility/diffusivity of Na^+ and increase its retention in the interface where there are more water molecules[55]. Meanwhile, as the water molecules dissociate in gel layer and reactions such as network-hydrolysis/condensation/ion-exchange/inter-diffusion occur, Na^+ ions in bulk gel layer become more mobile and are able to migrate within the gel layer or towards the surface to form precipitates.

The next important result to address is the boron loss and boron recondensation in vapor phase. Boron loss is evidenced through the ToF-SIMS profiles (87–91% loss) on the monolith samples. For the powder samples, the change in the ratio of BO_4/BO_3 in altered samples compared to the pristine samples signify a loss of boron, although not quantified.

In this study, there was an extremely small amount of water condensation on the glass powders altered in vapor phase. It is unclear if the water condensation on glass powders happened during the experiment or at the end of the experiment while cooling down the reactors to room temperature. Therefore, there is a possibility that at least some of the boron might have been leached out into the solution, especially for the powder samples. There did not seem to be any water condensation on the monolith samples altered in the same reactor. The reason behind the water condensation in vapor hydration experiments, only on powders and not on monoliths, could be the high surface area of the glass powders.

Many vapor hydration studies on borosilicate glasses have shown the loss of boron from the gel layer through ToF-SIMS profiles on glass monoliths[27,29,30]. Zhang et al. showed the conversion of $^{[4]}$B to $^{[3]}$B species and the formation of B-$(OH)_3$ species due to the hydrolysis of trigonal $^{[3]}$B network formers. Orthoboric and metaboric species can be volatile, especially at higher temperatures (>40 °C) and humidity[27,50,51]. Therefore, the evaporation of boric acid could be at least one of the mechanisms of boron loss from the gel layer during vapor hydration. This leads to some more questions regarding the limits to boric acid evaporation from gel layer with regards to time/temperature/vapor pressure/transport through gel layer/quantity of boron that could be lost through boric acid volatility etc.

Loss of boron through evaporation during aqueous alteration experiments has not been reported. A reasonable hypothesis is that boron loss by evaporation is more favored from a solid surface to vapor phase (sublimation) rather than from a liquid surface. Boric acid is soluble in water. The solubility limit of boric acid is 275 g L^{-1} at 100 °C[56]. It is very likely that B-$(OH)_3$ species volatilize as they are formed on monoliths altered in vapor phase and there is not sufficient quantity of water to dissolve boric acid. As the water quantity increases, boric acid dissolves in solution and therefore is not transported by vapor.

Regarding boron recondensation in the gel layer, the presence of B-^{17}O-B and Si-^{17}O-B species in the gel layer formed in vapor phase confirms boron recondensation, at least on the powder samples altered in vapor phase. The monolith samples altered in vapor phase only show evidence for loss of boron, but perhaps it is also possible that the 9–13% boron retained in the gel layer of the monolith samples are in fact recondensed boron. Another possibility is that the water condensation on the powders during vapor phase experiments might have inhibited boron loss by evaporation, but insufficient to leach out the boron. As a result, boron recondensation might have occurred only in the powder samples.

The global structure of gel layer formed in the two media are compared in the following paragraphs

Even though based on NMR spectroscopy results, the VP and AM systems seem overall similar, there are some differences to be noted.

(i) According to the quantity of hydrated boron species in the altered sample, the VP samples have a higher fraction of the

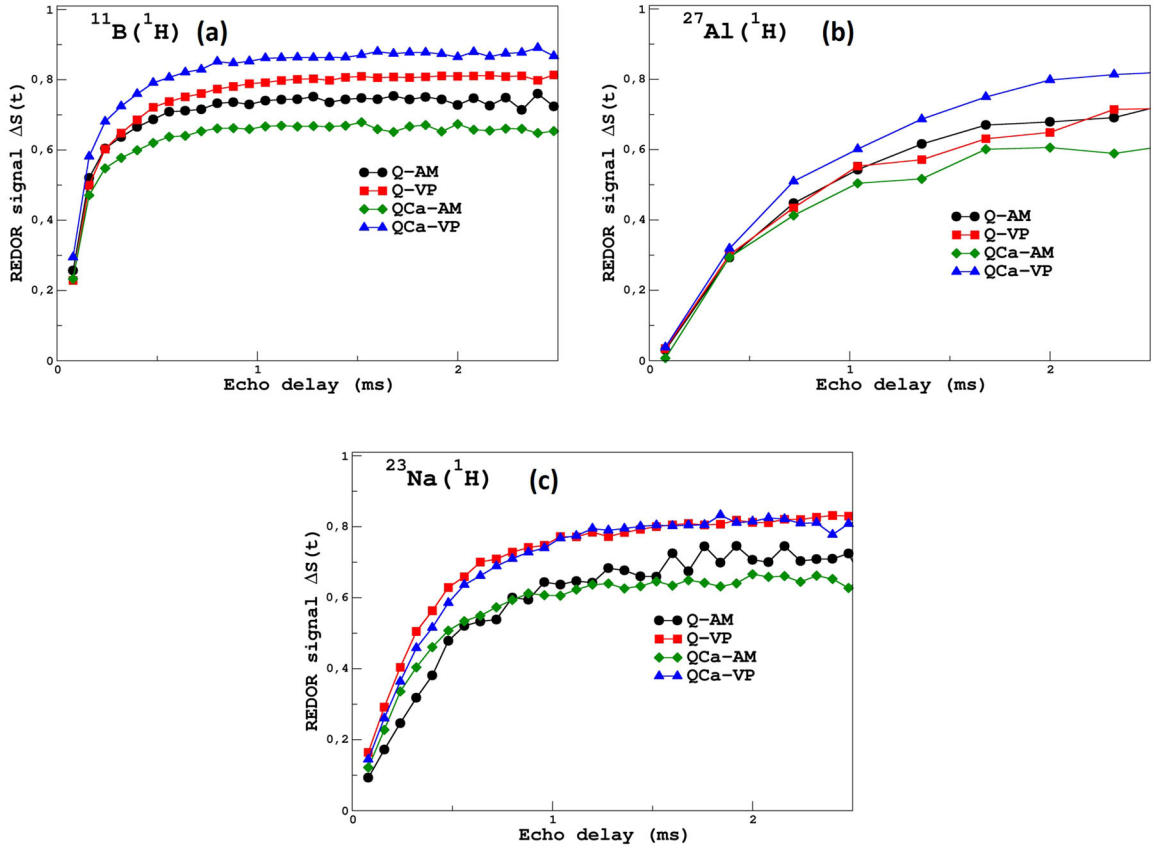

Fig. 8 REDOR NMR. REDOR ΔS(t) curves for the altered glass samples Q-AM, Q-VP, QCa-AM and QCa-VP; **a** ^{11}B{^{1}H} REDOR Δ*S*(*t*) curves; **b** ^{27}Al{^{1}H} REDOR Δ*S*(*t*) curves; **c** ^{23}Na{^{1}H} REDOR Δ*S*(*t*) curves.

hydrated species than the AM samples (as shown by REDOR NMR experiments). This is true for the hydrated Na species as well. This can be interpreted in two ways. One is that the gel layer formed in vapor phase is thicker and the other one is that the gel layer formed in vapor phase retains more water molecules. The former explanation is more likely. It is also supported by the fact that alteration kinetics show that QCa-VP has a thicker altered layer than QCa-AM for the same duration of alteration and Q-VP was anyway altered for a much longer duration than Q-AM. Therefore, the rate/degree of alteration of the VP samples is greater than the AM samples. This is confirmed by the REDOR NMR experiments and shows the potential of this technique to eventually be calibrated to calculate the glass alteration rate.

(ii) According to the REDOR NMR results, among the AM samples, Q is more hydrated; and among the VP samples QCa is slightly more hydrated, i.e., in aqueous medium, the glass Q alters faster than QCa and in vapor phase QCa alters at a slightly faster rate than Q. This shows that despite the doubts regarding water condensation on powder samples of Q-VP and QCa-VP, both the monolith and the powder samples altered in vapor phase follow the same trend where the glass QCa is slightly more altered than the glass Q.

(iii) Evidence for recondensation of boron with ^{17}O species is conclusively found only for VP samples. It is not surprising that boron did not recondense with ^{17}O in the gel layer formed in aqueous medium since boron recondensation was not reported before despite the many glass alteration studies in aqueous medium. The recondensation of Si and Al in aqueous medium is attributed to the solubility of the dissolving glass species and boron does not recondense in aqueous medium due to relatively higher solubility in water.

There is also evidence of recondensation of Na with ^{17}O in the QCa-VP sample, but not of recondensation of Ca. Alloteau et al. suggested that during the alteration of glasses in vapor phase, NBO sites (Si-O^{-}Na^{+}) may actually play a catalytic role, resulting in the recondensation of Na with ^{17}O from the water (refer to the three step reaction process given in the reference)[57]. Since Ca^{2+} is ionically bonded to two NBO sites on average, it might be difficult or might require more water molecules for such a recondensation reaction to occur. Moreover, Ca^{2+} is less retained than Na^{+} in the gel layer formed in vapor phase and Ca^{2+} has a tendency to form secondary phases such as calcite during vapor hydration[27,57]. It is not clear why Na^{+} does not recondense with ^{17}O in the Q-VP sample. It was already hypothesized that the loss of elements from the hydrated layer formed in vapor phase might trigger a reorganization of the hydrated layer into a gel layer. The catalytic role played by the NBO sites might also be a result of the reorganization of the gel layer due to loss of elements. In QCa-VP there is a significant loss of boron as well as Ca, whereas in Q-VP there is only a significant loss of B. Therefore, there might not be enough reorganization activity in the Q-VP gel layer to promote the recondensation of Na with ^{17}O.

(iv) In the Q-VP sample, there is a higher fraction of Si-^{17}O-Si than Si-^{17}O-Al, whereas the Si-^{17}O-Si and the Si-^{17}O-Al proportions are comparable in the Q-AM sample and the pristine Q glass. One of the hypotheses that can be put forward is that in vapor phase, the $[AlO_4]^{-}$ entities may be less soluble/hydrolysable by the water molecules from the vapor phase than the Si tetrahedral units. As a result, fewer Al atoms might have hydrolyzed and recondensed with ^{17}O than Si atoms.

In the QCa-VP sample on the other hand, the fraction of Si-^{17}O-Al is higher than the Si-^{17}O-Si. This could be due to the precipitation of zeolites containing Si and Al.

The below paragraphs discuss the differences between glass alteration in vapor phase and aqueous medium

In this study, the results have shown that glass alteration in vapor phase gave different alteration kinetics, different behavior of elements in the gel layer and different structure of altered layer than the glass alteration in aqueous medium. These differences are probably due to different rate-controlling mechanisms with time of alteration.

Based on the fact that only a very small amount of water is available for glass to react with in vapor phase, it could be considered that glass alteration in vapor phase could be similar to glass alteration in aqueous medium at an extremely high SA/V ratio. However, some studies have argued that glass alteration in vapor phase is distinct to glass alteration in aqueous medium because of some vapor-phase alteration mechanisms like "glass hydration without dealkalization," which were not encountered in studies of glass alteration in aqueous medium and other aqueous alteration mechanisms like "repolymerization," which have not yet been observed in vapor phase conditions. It has been suggested that the chemical properties of the glass-water system are modified with the alteration conditions[58,59]. Nevertheless, the understanding gained on aqueous alteration of glasses has been useful to understand glass alteration in vapor phase.

Based on the results in this study, the following hypotheses for a mechanism of gel layer formation in the vapor phase could be put forth. There is a hydration mechanism without loss of elements that first occurs at the glass-vapor interface forming a hydrated layer next to the pristine glass. This hydration mechanism could simply be penetration of water molecules. As the thickness of this hydrated layer increases, the structure of hydrated layer that is towards the vapor phase reorganizes into a gel-layer. This may be driven by water dissociation into H^+ and OH^- species at the surface and in the gel layer and its progression into the hydrated layer by means of interdiffusion and hydrolysis mechanisms, the loss of boron as $B(OH)_3$ and other elements migrating to form secondary phases. In other words, the interaction of the hydrated layer with the vapor phase promotes its reorganization into a gel layer and the hydrated layer that is close to the pristine glass remains as such for at least a few tens of nm. This proposed mechanism for gel-layer formation in vapor phase is different from the different models proposed for gel layer formation in aqueous medium.

It is not possible, with the available information, to explain the differences between glass alteration in the two media as an effect of increasing SA/V ratio alone. Vapor hydration is a dynamic process with a continuous supply of "pure/fresh" water molecules in contrast to a static AM experiment with a very small volume of water.

The possibility that the solvation properties of the adsorbed/bound water molecules may be different than that of liquid water[58] must be considered. These questions make it more challenging to use tools such as geochemical modeling to predict glass alteration rates in vapor phase.

To recapitulate this study and the main results, a quaternary Na-alumino-borosilicate glass and the same glass doped with CaO were altered in vapor phase and aqueous medium at a very high SA/V ratio. For the same duration of alteration, the Ca-doped glass altered more in vapor phase than in aqueous medium. For alteration in vapor phase, the Ca-doped glass altered slightly more than the non-doped glass. The two possible reasons hypothesized are: (i) Precipitation of zeolites increased the alteration rate or (ii) Network-hydrolysis is the predominant rate-controlling vapor hydration mechanism, which resulted in the less polymerized glass (the Ca-doped glass) being the more altered one. For alteration in aqueous medium, the Ca-doped glass altered less than its non-doped counterpart, probably due to the formation of a more passivating gel layer.

During vapor hydration of powders, there is also evidence for recondensation of boron, Si, Al and Na with ^{17}O isotopes supplied by the vapor phase. Boron is also lost in the gel layer formed during vapor hydration. It seems that one of the possible mechanisms for boron loss could be the evaporation of $B\text{-}(OH)_3$ species formed by the hydrolysis of trigonal BO_3 species.

There are some aspects revealed in this vapor hydration study that merit to be probed further with more meticulous experimentation and characterization such as the possibility of water condensation on glass powders vs. the dry appearance of monoliths and the quantification of boron evaporation from glass powders. These could provide insights into differences between glass alteration in vapor phase and aqueous medium and vapor hydration mechanisms.

METHODS

Glass synthesis

The glasses that were altered in vapor phase and aqueous medium were unenriched glasses. i.e. glasses of natural isotopic abundance. These glasses were altered in a medium enriched (40%) in ^{17}O isotope and were characterized by NMR spectroscopy to study the local environment of oxygen (^{17}O) atom incorporated into the gel layer. In order to compare the oxygen environment in the gel layer and in the pristine glass, pristine glasses enriched in ^{17}O isotope (80%) of same theoretical composition were synthesized and characterized by NMR spectroscopy.

Synthesis of unenriched glasses using oxide precursors

Approximately 200 g of the glasses were synthesized by heating the oxide precursors (SiO_2, H_3BO_3, Na_2CO_3, Al_2O_3 (and CaO for QCa)) in a Pt-Rh crucible for 3 h at 1450 °C and annealing them in a graphite crucible for 1 h at 620 °C. After 1 h of annealing, the temperature of the furnace was decreased to 300 °C at a rate of 0.5 °C min^{-1} and then it was turned off. The glass blocks thus obtained were cut to make optically polished monoliths (surface roughness <1 µm) of dimensions ($2.5 \times 2.5 \times 0.1$ cm^3) and the remaining glass pieces were then crushed with tungsten carbide balls in a Retsch MM400 ball-mill apparatus to obtain glass powder. Glass powders of particle size $0.45 < ø < 2$ µm were obtained by decantation (application of Stokes' law for terminal velocity of glass particles of 1 micron radius falling through 99.99% pure acetone solvent and using 0.45 µm pore-size membrane filter). A small quantity of the glass powders was dissolved in an acid solution (10 HCl + 5 HNO_3 + 4 HF) and their compositions were analyzed using Inductively Coupled Plasma –Optical Emission Spectroscopy (ICP-OES) (Thermo Scientific iCAPTM 6000 series) (composition in mol% of oxides, Q: 57.5 SiO_2–15.3 B_2O_3–19.2 Na_2O–8.1 Al_2O_3; QCa: 52.7 SiO_2–14.6 B_2O_3–19 Na_2O–7.5 Al_2O_3–6.2 CaO). The density of the glass Q and QCa as measured by the He pycnometer was 2.44 g cm^{-3} and 2.5 g cm^{-3}, respectively. The specific surface area of the Q and QCa glass powders as measured by BET was 5 m^2 g^{-1} and 4.64 m^2 g^{-1}, respectively.

Synthesis of glasses via sol-gel method (alkoxide precursors). Two batches (200 mg each) of the Q and QCa glasses were prepared using a sol–gel process. Metal-alkoxide precursors ($Si(C_2H_5O)_4$, $B(C_2H_5O)_3$, $Al(C_2H_5O)_3$, $NaOC_2H_5$ (and Ca $(CH_3O)_2$ for QCa)) were mixed with anhydrous C_2H_5OH and stoichiometric proportion of enriched water (80% ^{17}O) according to Eq. (1) in one batch and water of natural abundance in the second (reference) batch.

$$M-(O-R)+n\,H_2\,{}^{17}O \rightarrow M\left({}^{17}OH\right)_n + n\,ROH \quad (1)$$

(In Eq. (1), M = metal of charge n^+; R = organic group)

After hydrolysis reactions, wet-gels were formed, which were then dried in an oven at 90 °C. These well-mixed powdered dry-gels were then melted in two separate platinum foils in an oven, under argon atmosphere. The powders were subjected to a dehydration step at 160 °C for 1 h and then the temperature of the oven was raised to 1200 °C at a rate of 4.7 °C min^{-1} and the glasses were melted at this temperature for 25 min. The platinum

foils are then immediately removed from the oven and glassy masses form almost instantaneously upon rapid cooling. The resulting glasses were crushed in a Retsch MM200 ball-mill apparatus to obtain glass powders. The first batch containing ^{17}O enriched glasses was used for NMR spectroscopy experiments and the second batch containing natural abundance glasses was analyzed for chemical composition using ICP-OES spectroscopy (composition in mol% of oxides, Q: 64.3 SiO_2–10.3 B_2O_3–16.4 Na_2O–9.1 Al_2O_3; QCa: 58.1 SiO_2–8.3 B_2O_3–15.3 Na_2O–8.8 Al_2O_3–9.5 CaO). The differences in composition between the unenriched glasses and the glasses enriched in ^{17}O are due to the evaporation of boron and sodium oxides during melting. However, according to the comparison of the NMR spectra of both glasses, the glass structural characteristics are quite similar.

Glass alteration protocols

Aqueous alteration. Experiments 1 to 4 in Table 1 describe the glass alteration experiments in aqueous medium. Approximately, 250 mg of Q and QCa glass powders ($0.45 < ø < 2$ µm) were leached by 2.22 g and 2.06 g of 40% $H_2{}^{17}O$ enriched DI water respectively in PFA containers to achieve very high SA/V ratios of 570,440 m^{-1} and 563,710 m^{-1}, respectively (experiments 1 and 3, respectively). 40% $H_2{}^{17}O$ enriched DI water is also enriched in ^{18}O. The first PFA container was placed in a second larger PFA container with water to minimize water loss. This setup was placed in an oven at 90 °C. The glass Q was altered for 59 days and the glass QCa was altered for 213 days. At the end of the experiment, the pH of the solution was measured, and the leachate was sampled, ultra-filtered using a 10000 Dalton membrane filter (~2 nm) and diluted in 0.5 N HNO_3 and analyzed using ICP-OES to calculate the altered glass fraction.

A duplicate experiment was carried out for each glass using DI water of natural isotopic abundance (experiments 2 and 4). Refer to Table 1 for sample masses and SA/V ratio. 100 µL of leachate was periodically sampled to follow alteration kinetics. This precaution was taken to monitor the evolution of glass alteration and prevent the possible formation of a large quantity of secondary phases at high SA/V ratio and temperature conditions that may destabilize the gel due to formation of zeolites, as observed in literature[52,60,61].

The concentrations of the elements of interest (Si, B, Na, Ca, Al) were analyzed by ICP-OES. The rate of glass alteration corresponds to the slope of the evolution of the Normalized mass Loss of boron (usually boron is considered as a tracer since it is highly soluble and is not usually retained in gel layer or in secondary phases, but only in the gel–glass interface[11,38]) (NL in g m^{-2}) with respect to time[62]. NL is calculated using the Eq. (2) as shown below:

$$\mathrm{NL}(i) = \frac{C(i)}{\frac{SA}{V} * x(i)} \tag{2}$$

i denotes the element; C denotes the concentration of the element at a given time in g m^{-3}; SA/V is the surface area of glass to solution volume ratio in m^{-1}; x denotes the mass fraction of the element in glass.

The equivalent thickness of altered glass (E_{eq}) can be calculated depending on sample geometry. For glass powders, (E_{eq}) can be calculated using the Eqs. (3)–(5).

$$E_{eq} = \left(1 - (1 - \mathrm{AGf})^{\frac{1}{3}}\right) * R_0 \tag{3}$$

$$R_0 = \frac{3}{\rho * S_S} \tag{4}$$

$$\mathrm{AGf} = \frac{C(B)_t * V_t + \sum_{j=1}^{t-1} C(B)_j * V_{s_j}}{m_0 * x(B)} \tag{5}$$

AGf is the fraction of altered glass calculated from boron concentration; R_0 is the initial glass grain radius in m; S_S is the specific surface area of glass powders in $m^2\ g^{-1}$; V_t is the leachate volume at time t in m^3; V_{s_j} is the volume sampled at time j in m^3; m_0 is the initial mass of glass powders in g; ρ is the density of glass in g m^{-3}.

Vapor phase hydration. Approximately 300 mg of Q and QCa glass powders ($0.45 < ø < 2$ µm) (experiments 5 and 7, respectively) with natural abundance of oxygen were each taken in a PTFE cup placed in a PTFE container. 3.25 wt% of NaCl was prepared using 40% $H_2{}^{17}O$ enriched water and added at the bottom of each container to impose 98% relative humidity (RH) at 90 °C [63]. After alteration, these powders were characterized by NMR spectroscopy to study the global structure of the gel layer that incorporates ^{17}O isotopes from the vapor phase. A ($2.5 \times 2.5 \times 0.1$ cm^3) monolith of each glass (experiments 6 and 8) was also placed above the NaCl solution in the same reactor, to analyze the thickness of the altered layer formed using Scanning Electron Microscope (SEM) and study the behavior of elements in the gel layer by Time of Flight-Secondary Ion Mass Spectrometry (ToF-SIMS). This set-up was placed inside a stainless-steel autoclave, which was in-turn placed inside an aluminum over-container to avoid rapid heating and cooling of the reactor set-up. The entire vapor phase alteration protocol is based on the protocol used in the cited refs. [25,26,28–30]. The two reactors, each containing the Q and QCa samples respectively, were placed in an oven at 90 °C for 213 days. These durations were adapted to obtain a significant proportion of gel in the altered powders. At the end of the experiment, the reactors were cooled to ambient conditions and the samples were retrieved and stored in aluminum foils/Eppendorf tubes in ambient conditions until characterization.

The altered samples were characterized using SEM (Zeiss Gemini Supra 55, JEOL JSM 6330 F), X-Ray Diffraction (XRD, Philips X'Pert diffractometer) and ToF-SIMS (SSIMS ON TOF 5 – IONTOF). For the ToF-SIMS analysis, $Bi_1{}^+$ primary ions at 25 KeV and 1.5 pA were used for the analysis cycles of secondary positive ions. $Bi_3{}^{++}$ primary ions at 25 KeV and 0.03 pA were used for the analysis cycles of secondary negative ions. Area analyzed was 50×50 µm^2. Surface neutralization was carried out using electron pulse at low energy (<20 eV). $O_2{}^+$ primary ions at 1 KeV and 300 nA were used for the abrasion cycles of secondary positive ions. Cs^+ primary ions at 1 KeV and 60 nA were used for the abrasion cycles of secondary negative ions. The area eroded was 250×250 µm^2.

At the end of the analysis, the depth of the crater (portion of the sample analyzed) is measured using a mechanical profilometer and is used for depth calibration. Thus, at the end of the analysis, we obtain the intensities of different elements as a function of the depth of the sample analyzed (depth profiles). The profiles were normalized with respect to the intensity of each element (C) in the pristine glass (denoted as PG) and with respect to the intensity of Si (C_{Si}) at given depth as shown in the Eq. (6) below.

$$\text{Normalized intensity} = \frac{\frac{C}{C_{Si}}}{\left(\frac{C}{C_{Si}}\right)_{PG}} \tag{6}$$

$$\text{Altered layer depth} = x_0 \text{ at which } \left(0.5 - \frac{\frac{C_B}{C_{Si}}}{\left(\frac{C_B}{C_{Si}}\right)_{PG}} = 0\right) \tag{7}$$

In many vapor hydration studies, boron is the element that is the most depleted in the altered layer (in depth and in quantity)[25,27,29,31,37,50]. Retention of boron in the gel layer is often less than 10–20%. Therefore, it is used as a tracer to calculate the depth of the altered layer using Eq. (7).

Often, the depth of hydrogen penetration is compared to the thickness of boron depletion during vapor hydration. The hydrogen penetration depth is calculated from the ToF-SIMS profiles using Eq. 8 as shown below. The $C_{H_{(\text{avg. Gel layer})}}$ refers to the average of the normalized H intensity in the gel layer. Similarly, the depth of penetration of ^{17}O and ^{18}O are also studied. These depths are also calculated using Eq. (8) by replacing $C_{H_{(\text{avg. Gel layer})}}$ with $C_{18\,or\,17_{O(\text{avg. gel layer})}}$.

Depth (x) of hydrogen penetration is the depth at which the normalized H intensity is equal to a value calculated using the Eq. (8) given below.

$$\text{Normalized } H \text{ intensity} = \frac{C_{H_{(\text{avg. gel layer})}} + 1}{2} \quad (8)$$

NMR spectroscopy

NMR data were collected on a Bruker 500WB Avance II spectrometer operating at a magnetic field of 11.72 T, using a 4-mm Bruker CP-MAS probe at a spinning frequency of 12.5 kHz. For ^{27}Al, ^{23}Na and ^{11}B, a short single pulse excitation of 1 µs in length (tip angle of about 15°–20°) was used to acquire quantitative spectra with a recycle delay of 1 s for ^{27}Al, ^{23}Na and 2 s for ^{11}B. ^{17}O MAS NMR spectra were acquired using a rotor-synchronized spin echo pulse sequence (i.e., with a spin echo delay of one rotor period and soft selective pulses on the central transition) in order to minimize the baseline distortion due to the ringing signal. For ^{17}O two-dimensional multiple quantum MAS (MQMAS) spectra, the Z-filter three pulse sequence[64] was used. For ^{11}B MQMAS experiments, Z-filter and RIACT two pulse sequence were used for optimized acquisition of the BO_4 and BO_3 peaks, respectively, as detailed in Refs. [15,65]. ^{29}Si MAS NMR spectra were acquired using a 90° pulse after a presaturation period (composed of a train of about twenty 90° pulses with a 2 ms delay between the pulses) and a recycle delay of 20 s (no change in lineshape were observed for longer recycle delay). For REDOR experiments soft selective 90° and 180° pulses (radio frequency 10–20 kHz; 180° pulse duration of 8–10 µs) were applied on the central transition (1/2 ↔ 1/2) of the observed nucleus (here ^{11}B, ^{23}Na and ^{27}Al), and a rotor-synchronized train of 180° pulses of 9 µs in length for ^{1}H[49,66,67]. Chemical shifts are referenced to an external sample of 1 M boric acid solution (19.6 ppm) for ^{11}B, 1 M $AlCl_3$ solution (0 ppm) for ^{27}Al, 1 M NaCl solution (0 ppm) for ^{23}Na, powder tetrakistrimethylsilane (TKS) with the highest intensity peak situated at −9.9 ppm (from that of TMS) for ^{29}Si and at 0.2 ppm for ^{1}H, and $H_2{}^{17}O$ (enrichment 40%, 0 ppm). We observed that ^{1}H decoupling did not impact the resolution of the spectra for all observed nuclei, suggesting that the MAS spinning frequency was high enough to average out ^{1}H-X dipolar couplings in our altered samples. All data were processed and fitted using in-house software (T. Charpentier) with procedures described in refs. [15,65,68].

DATA AVAILABILITY

The SEM data supporting the findings are available within the article and the supplementary information. The treated data of ToF-SIMS, NMR spectroscopy and XRD are also available within the article and supplementary information. The raw data of ToF-SIMS, NMR spectroscopy, and XRD required to reproduce these findings cannot be shared within the article. However, they can be shared by the corresponding author upon reasonable request.

Received: 21 February 2022; Accepted: 16 October 2022;
Published online: 04 November 2022

REFERENCES

1. ANDRA-Collectif. Dossier d'Options de Sûreté - Partie Après Fermeture (DOS-AF) (Agence Nationale Pour La Gestion Des Dechets Radioactifs, 2016).
2. Gin, S. et al. An international initiative on long-term behavior of high-level nuclear waste glass. *Mater. Today* **16**, 243–248 (2013).
3. Gin, S., Beaudoux, X., Angéli, F., Jégou, C. & Godon, N. Effect of composition on the short-term and long-term dissolution rates of ten borosilicate glasses of increasing complexity from 3 to 30 oxides. *J. Non-Cryst. Solids* **358**, 2559–2570 (2012).
4. Mir, A. H. et al. Effect of decades of corrosion on the microstructure of altered glasses and their radiation stability. *npj Mater. Degrad.* **4**, 11 (2020).
5. Bouakkaz, R., Abdelouas, A., El Mendili, Y., Grambow, B. & Gin, S. SON68 glass alteration under Si-rich solutions at low temperature (35–90 °C): kinetics, secondary phases and isotopic exchange studies. *RSC Adv.* **6**, 72616–72633 (2016).
6. Angeli, F., Gaillard, M., Jollivet, P. & Charpentier, T. Influence of glass composition and alteration solution on leached silicate glass structure: a solid-state NMR investigation. *Geochim. Cosmochim. Acta* **70**, 2577–2590 (2006).
7. Lenting, C. et al. Towards a unifying mechanistic model for silicate glass corrosion. *npj Mater. Degrad.* **2**, 28 (2018).
8. Gin, S., Delaye, J.-M., Angeli, F. & Schuller, S. Aqueous alteration of silicate glass: state of knowledge and perspectives. *npj Mater. Degrad.* **5**, 42 (2021).
9. Thorpe, C. L. et al. Forty years of durability assessment of nuclear waste glass by standard methods. *npj Mater. Degrad.* **5**, 61 (2021).
10. Valle, N. et al. Elemental and isotopic (^{29}Si and ^{18}O) tracing of glass alteration mechanisms. *Geochim. Cosmochim. Acta* **74**, 3412–3431 (2010).
11. Gin, S. et al. The controversial role of inter-diffusion in glass alteration. *Chem. Geol.* **440**, 115–123 (2016).
12. Gin, S. et al. A general mechanism for gel layer formation on borosilicate glass under aqueous corrosion. *J. Phys. Chem. C* **124**, 5132–5144 (2020).
13. Verney-Carron, A. et al. Understanding the mechanisms of Si–K–Ca glass alteration using silicon isotopes. *Geochim. Cosmochim. Acta* **203**, 404–421 (2017).
14. Gin, S. et al. Origin and consequences of silicate glass passivation by surface layers. *Nat. Commun.* **6**, 6360 (2015).
15. Hopf, J. et al. Glass–water interaction: effect of high-valence cations on glass structure and chemical durability. *Geochim. Cosmochim. Acta* **181**, 54–71 (2016).
16. Hopf, J. et al. Toward an understanding of surface layer formation, growth, and transformation at the glass–fluid interface. *Geochim. Cosmochim. Acta* **229**, 65–84 (2018).
17. Bunker, B. C. Molecular mechanisms for corrosion of silica and silicate glasses. *J. Non-Cryst. Solids* **179**, 300–308 (1994).
18. Frugier, P., Chave, T., Gin, S. & Lartigue, J.-E. Application of the GRAAL model to leaching experiments with SON68 nuclear glass in initially pure water. *J. Nucl. Mater.* **392**, 552–567 (2009).
19. Gin, S. et al. Can a simple topological-constraints-based model predict the initial dissolution rate of borosilicate and aluminosilicate glasses? *npj Mater. Degrad.* **4**, 6 (2020).
20. Arab, M. et al. Aqueous alteration of five-oxide silicate glasses: experimental approach and Monte Carlo modeling. *J. Non. Cryst. Solids* **354**, 155–161 (2008).
21. Anoop Krishnan, N. M. et al. Predicting the dissolution kinetics of silicate glasses using machine learning. *J. Non-Cryst. Solids* **487**, 37–45 (2018).
22. Oey, T. et al. The role of the network-modifier's field-strength in the chemical durability of aluminoborate glasses. *J. Non-Cryst. Solids* **505**, 279–285 (2019).
23. Mascaraque, N., Bauchy, M. & Smedskjaer, M. M. Correlating the network topology of oxide glasses with their chemical durability. *J. Phys. Chem. B* **121**, 1139–1147 (2017).
24. Bauchy, M. Deciphering the atomic genome of glasses by topological constraint theory and molecular dynamics: a review. *Comput. Mater. Sci.* **159**, 95–102 (2019).
25. Abdelouas, A. et al. A preliminary investigation of the ISG glass vapor hydration. *Int. J. Appl. Glas. Sci.* **4**, 307–316 (2013).
26. Ait Chaou, A. et al. Vapor hydration of a simulated borosilicate nuclear waste glass in unsaturated conditions at 50 °C and 90 °C. *RSC Adv.* **5**, 64538–64549 (2015).
27. Narayanasamy, S. et al. Influence of composition of nuclear waste glasses on vapor phase hydration. *J. Nucl. Mater.* **525**, 53–71 (2019).
28. Ait Chaou, A., Abdelouas, A., El Mendili, Y. & Martin, C. The role of pH in the vapor hydration at 175 °C of the French SON68 glass. *Appl. Geochemistry* **76**, 22–35 (2017).
29. Neeway, J. et al. Vapor hydration of SON68 glass from 90 °C to 200 °C: a kinetic study and corrosion products investigation. *J. Non-Cryst. Solids* **358**, 2894–2905 (2012).
30. Bouakkaz, R., Abdelouas, A. & Grambow, B. Kinetic study and structural evolution of SON68 nuclear waste glass altered from 35 to 125 °C under unsaturated H2O and D2O18 vapour conditions. *Corros. Sci.* **134**, 1–16 (2018).
31. Narayanasamy, S., Jollivet, P., Sessegolo, L., Angeli, F. & Abdelouas, A. Influence of temperature and relative humidity on vapor hydration of an AVM nuclear waste glass. *J. Nucl. Mater.* **543**, 152571 (2021).
32. Jegou, C., Narayanasamy, S. & Angeli, F. Short communication on the Influence of the temperature between 30 and 70 °C on the hydration of SON68 nuclear waste glass in a vapour phase. *J. Nucl. Mater.* **545**, 152738 (2021).

33. Chave, T., Frugier, P., Gin, S. & Ayral, A. Glass–water interphase reactivity with calcium rich solutions. *Geochim. Cosmochim. Acta* **75**, 4125–4139 (2011).
34. Mercado-Depierre, S., Angeli, F., Frizon, F. & Gin, S. Antagonist effects of calcium on borosilicate glass alteration. *J. Nucl. Mater.* **441**, 402–410 (2013).
35. Jollivet, P., Gin, S. & Schumacher, S. Forward dissolution rate of silicate glasses of nuclear interest in clay-equilibrated groundwater. *Chem. Geol.* **330–331**, 207–217 (2012).
36. Tangari, A. C., Marinangeli, L., Scarciglia, F., Pompilio, L. & Piluso, E. Volcanic holocrystalline bedrock and hydrothermal alteration: a terrestrial analogue for Mars. *Minerals* **10**, 1082 (2020).
37. Narayanasamy, S. *Influence of Composition on Vapor Hydration of AVM Nuclear Glasses. Material Chemistry* (Ecole Nationale Supérieure Mines-Télécom Atlantique, 2019).
38. Aréna, H. et al. Characterization of the boron profile and coordination in altered glass layers by EEL spectroscopy. *Micron* **141**, 102983 (2021).
39. Angeli, F., Charpentier, T., Gin, S. & Petit, J. C. 17O 3Q-MAS NMR characterization of a sodium aluminoborosilicate glass and its alteration gel. *Chem. Phys. Lett.* **341**, 23–28 (2001).
40. Aréna, H. et al. Impact of Fe, Mg and Ca elements on glass alteration: Interconnected processes. *Geochim. Cosmochim. Acta* **239**, 420–445 (2018).
41. Aréna, H., Rébiscoul, D., Garcès, E. & Godon, N. Comparative effect of alkaline elements and calcium on alteration of International Simple Glass. *npj Mater. Degrad.* **3**, 10 (2019).
42. Angeli, F., Charpentier, T., Gaillard, M. & Jollivet, P. Influence of zirconium on the structure of pristine and leached soda-lime borosilicate glasses: towards a quantitative approach by 17O MQMAS NMR. *J. Non-Cryst. Solids* **354**, 3713–3722 (2008).
43. Krisnandi, Y. K. et al. Synthesis and characterization of crystalline NaY-zeolite from Belitung Kaolin as catalyst for n-hexadecane cracking. *Crystals* **9**, 404 (2019).
44. Engelhardt, G. & Michel, D. *High-Resolution Solid-State NMR of Silicates and Zeolites* (Wiley, 1987).
45. Collin, M., Fournier, M., Charpentier, T., Moskura, M. & Gin, S. Impact of alkali on the passivation of silicate glass. *npj Mater. Degrad.* **2**, 16 (2018).
46. Oglesby, J. V., Zhao, P. & Stebbins, J. F. Oxygen sites in hydrous aluminosilicate glasses: the role of Al-O-Al and H_2O. *Geochim. Cosmochim. Acta* **66**, 291–301 (2002).
47. Seidel, A., Schimiczek, B., Tracht, U. & Boddenberg, B. ^{23}Na solid state MAS NMR of sodium halides occluded in zeolites. *Solid State Nucl. Magn. Reson.* **9**, 129–141 (1997).
48. Lim, K. H. & Clare, P. G. Characterization of extra-framework cation positions in zeolites NaX and NaY with very fast 23Na MAS and multiple quantum MAS NMR spectroscopy. *J. Am. Chem. Soc.* **122**, 9768–9780 (2000).
49. Angeli, F. et al. Effect of thermally induced structural disorder on the chemical durability of International Simple Glass. *npj Mater. Degrad.* **2**, 31 (2018).
50. Zhang, H., Suzuki-Muresan, T., Morizet, Y., Gin, S. & Abdelouas, A. Investigation on boron and iodine behavior during nuclear glass vapor hydration. *npj Mater. Degrad.* **5**, 10 (2021).
51. Balasubramanian, R., Lakshmi Narasimhan, T. S., Viswanathan, R. & Nalini, S. Investigation of the vaporization of boric acid by transpiration thermogravimetry and Knudsen effusion mass spectrometry. *J. Phys. Chem. B* **112**, 13873–13884 (2008).
52. Fournier, M., Gin, S., Frugier, P. & Mercado-Depierre, S. Contribution of zeolite-seeded experiments to the understanding of resumption of glass alteration. *npj Mater. Degrad.* **1**, 17 (2017).
53. Gin, S., Frugier, P., Jollivet, P., Bruguier, F. & Curti, E. New insight into the residual rate of borosilicate glasses: effect of S/V and glass composition. *Int. J. Appl. Glas. Sci.* **4**, 371–382 (2013).
54. Mercado-Depierre, S., Fournier, M., Gin, S. & Angeli, F. Influence of zeolite precipitation on borosilicate glass alteration under hyperalkaline conditions. *J. Nucl. Mater.* **491**, 67–82 (2017).
55. Jabraoui, H., Gin, S., Charpentier, T., Pollet, R. & Delaye, J.-M. Leaching and reactivity at the sodium aluminosilicate glass–water interface: insights from a ReaxFF Molecular Dynamics Study. *J. Phys. Chem. C* **125**, 27170–27184 (2021).
56. Vaghetto, R. et al. Experimental observations of boric acid precipitation scenarios. *Nucl. Eng. Des.* **312**, 422–428 (2017).
57. Alloteau, F. et al. Evidence for different behaviors of atmospheric glass alteration as a function of glass composition. *npj Mater. Degrad.* **4**, 36 (2020).
58. Majérus, O. et al. Glass alteration in atmospheric conditions: crossing perspectives from cultural heritage, glass industry, and nuclear waste management. *npj Mater. Degrad.* **4**, 27 (2020).
59. Collin, M. et al. Chemical durability of lead crystal glass: Comparison of short-term aqueous and atmospheric alteration at 90 °C. *Int. J. Appl. Glas. Sci.* **12**, 158–174 (2020).
60. Fournier, M., Gin, S. & Frugier, P. Resumption of nuclear glass alteration: state of the art. *J. Nucl. Mater.* **448**, 348–363 (2014).
61. Ribet, S. & Gin, S. Role of neoformed phases on the mechanisms controlling the resumption of SON68 glass alteration in alkaline media. *J. Nucl. Mater.* **324**, 152–164 (2004).
62. Ribet, I. & Godon, N. *Altération par l'eau des verres borosilicatés Exemple des verres nucléaires, Techniques de l'ingénieur, Matériaux: résistance à la corrosion et au vieillissement. COR450 v1* https://www.techniques-ingenieur.fr (2014).
63. Pitzer, K., Rogers, P. & Peiper, J. Thermodynamics of high temperature brines. *Lawrence Berkeley Lab. Nucl. Waste Isol. Geophys. Reserv. Eng. Geosci.* 152–154 (1982).
64. Massiot, D. et al. Two-dimensional magic-angle spinning isotropic reconstruction sequences for quadrupolar nuclei. *Solid State Nucl. Magn. Reson.* **6**, 73–83 (1996).
65. Angeli, F., Charpentier, T., De Ligny, D. & Cailleteau, C. Boron speciation in soda-lime borosilicate glasses containing zirconium. *J. Am. Ceram. Soc* **93**, 2693–2704 (2010).
66. Bertmer, M., Züchner, L., Chan, J. C. C. & Eckert, H. Short and medium range order in sodium aluminoborate glasses. 2. Site connectivities and cation distributions studied by rotational echo double resonance NMR spectroscopy. *J. Phys. Chem. B* **104**, 6541–6553 (2000).
67. Janssen, M. & Eckert, H. 11B{23Na} Rotational echo double resonance NMR: a new approach for studying the spatial cation distribution in sodium borate glasses. *Solid State Ionics* **136–137**, 1007–1014 (2000).
68. Collin, M. et al. Structure of International Simple Glass and properties of passivating layer formed in circumneutral pH conditions. *npj Mater. Degrad.* **2**, 4 (2018).

ACKNOWLEDGEMENTS

We would like to thank Jean-Pierre Mestre (CEA) and Marie Fenart (CEA) for the SEM images, Myriam Chartier (CEA) for XRD patterns, Laurent Dupuy and Elodie Chauvet (TESCAN Analytics) for the ToF-SIMS profiles, Géraldine Parisot (CEA) and FILAB for the ICP-OES solution concentration analysis. The study was financially supported by CEA and EDF (Electricité de France).

AUTHOR CONTRIBUTIONS

P.J., F.A., S.N. and T.C. conceptualized the experiments. S.N. and P.J. prepared the samples and conducted the glass alteration experiments. M.M. and T.C. conducted the NMR experiments. S.N. analyzed the glass leaching and vapor hydration data. T.C., F.A. and S.N. analyzed the NMR data. S.N. wrote the original draft with contributions from T.C. regarding the NMR experimental details, results, and interpretation. C.J. contributed to writing, review, and editing. P.J., F.A., and A.A. supervised the study. A.A., F.A. and T.C. additionally contributed to review and editing.

COMPETING INTERESTS

The authors declare no competing interests.

ADDITIONAL INFORMATION

Supplementary information The online version contains supplementary material available at https://doi.org/10.1038/s41529-022-00298-2.

Correspondence and requests for materials should be addressed to Sathya Narayanasamy, Thibault Charpentier or Frédéric Angeli.

Reprints and permission information is available at http://www.nature.com/reprints

Publisher's note Springer Nature remains neutral with regard to jurisdictional claims in published maps and institutional affiliations.